STATE OF ALASKA

DEPARTMENT OF NATURAL RESOURCES

DIVISION OF GEOLOGICAL AND GEOPHYSICAL SURVEYS

Bill Sheffield — *Governor*

Esther Wunnicke — *Commissioner*

Ross G. Schaff — *State Geologist*

April 1983

This report is a preliminary publication of DGGS. The author is solely responsible for its content and will appreciate candid comments on the accuracy of the data as well as suggestions to improve the report.

Report of Investigations 83-9
GEOLOGY AND MINERALIZATION OF THE SILVER FOX MINE, FAIRBANKS MINING DISTRICT, ALASKA

By
G.E. Sherman

STATE OF ALASKA
Department of Natural Resources
DIVISION OF GEOLOGICAL & GEOPHYSICAL SURVEYS

According to Alaska Statute 41, the Alaska Division of Geological and Geophysical Surveys is charged with conducting 'geological and geophysical surveys to determine the potential of Alaska lands for production of metals, minerals, fuels, and geothermal resources; the locations and supplies of ground waters and construction materials; the potential geologic hazards to buildings, roads, bridges, and other installations and structures; and shall conduct other surveys and investigations as will advance knowledge of the geology of Alaska.'

In addition, the Division shall collect, evaluate, and publish data on the underground, surface, and coastal waters of the state. It shall also file data from water-well-drilling logs.

DGGS performs numerous functions, all under the direction of the State Geologist---resource investigations (including mineral, petroleum, and water resources), geologic-hazard and geochemical investigations, and information services.

Administrative functions are performed under the direction of the State Geologist, who maintains his office in Anchorage (3001 Porcupine Dr., 99501, ph 274-9681).

This report is for sale by DGGS for $5. It may be inspected at any of the four DGGS information offices: Alaska National Bank of the North Bldg., Geist Rd. and University Ave., Fairbanks; 3601 C St. (10th Floor), Anchorage; 230 So. Franklin St. (4th Floor), Juneau; and the State Office Bldg., Ketchikan. Mail orders should be addressed to DGGS, P.O. Box 80007, College, AK 99708.

CONTENTS

FIGURES

Page

TABLES

PLATES

GEOLOGY AND MINERALIZATION OF THE SILVER FOX MINE, FAIRBANKS MINING DISTRICT, ALASKA

By
Gary E. Sherman

ABSTRACT

The Silver Fox Mine is located approximately 17 mi north of Fairbanks, Alaska, in a quartz diorite-granodiorite pluton that is in contact with two quartz monzonite stocks to the north. Alteration and mineralization events have produced a quartz-molybdenite stockwork, argentiferous galena-sphalerite-pyrite fissure veins, and minor gold-stibnite mineralization.

A model was developed that suggests that thermal collapse of the system ---associated with mineralization---caused overprinting of high-temperature phases by lower temperature phases.

The Silver Fox Mine appears to represent a weakly developed molybdenum-porphyry system of the granodiorite type as described by Mutschler and others (1981); grade is estimated to be far lower than that of currently economic stockworks. Potential for exploitation of the sulfide and gold veins is low because of discontinuous strike lengths and narrow widths, but small-scale mining of the high-grade lead-silver veins may be possible.

INTRODUCTION

Purpose

The purpose of this study was to examine both the structural and geologic controls of mineralization that occurs on the Silver Fox Mine property. A basic model was constructed to depict the sequence of alteration and mineralizing events. The presence of molybdenum in a quartz stockwork exposed underground has been related to a possible porphyry system (Mowatt, 1974). This possibility was examined in terms of alteration and geologic setting to determine if evidence supporting such a supposition was present. A qualitative evaluation of the production potential of the mine was made on the basis of information gained from the study.

Field work was conducted primarily during the summer of 1979 and spring of 1980.

Location and Description of Study Area

The Silver Fox Mine claims are located 2 mi east of the Elliot Highway, approximately 17 mi north of Fairbanks (fig. 1). The claim block consists of four federal and 13 state lode claims totalling 520 acres (pl. 1).

Rolling hills characterize the topography of the area, and elevations range from 1,300 to 2,200 ft above sea level. Most development work has been done on the divide between Fox and Flume Creeks. Underground workings consist of approximately 600 ft of headings and drifts and one shaft approximately 25 ft deep. Surface excavations are limited to pits and trenches in mineralized areas.

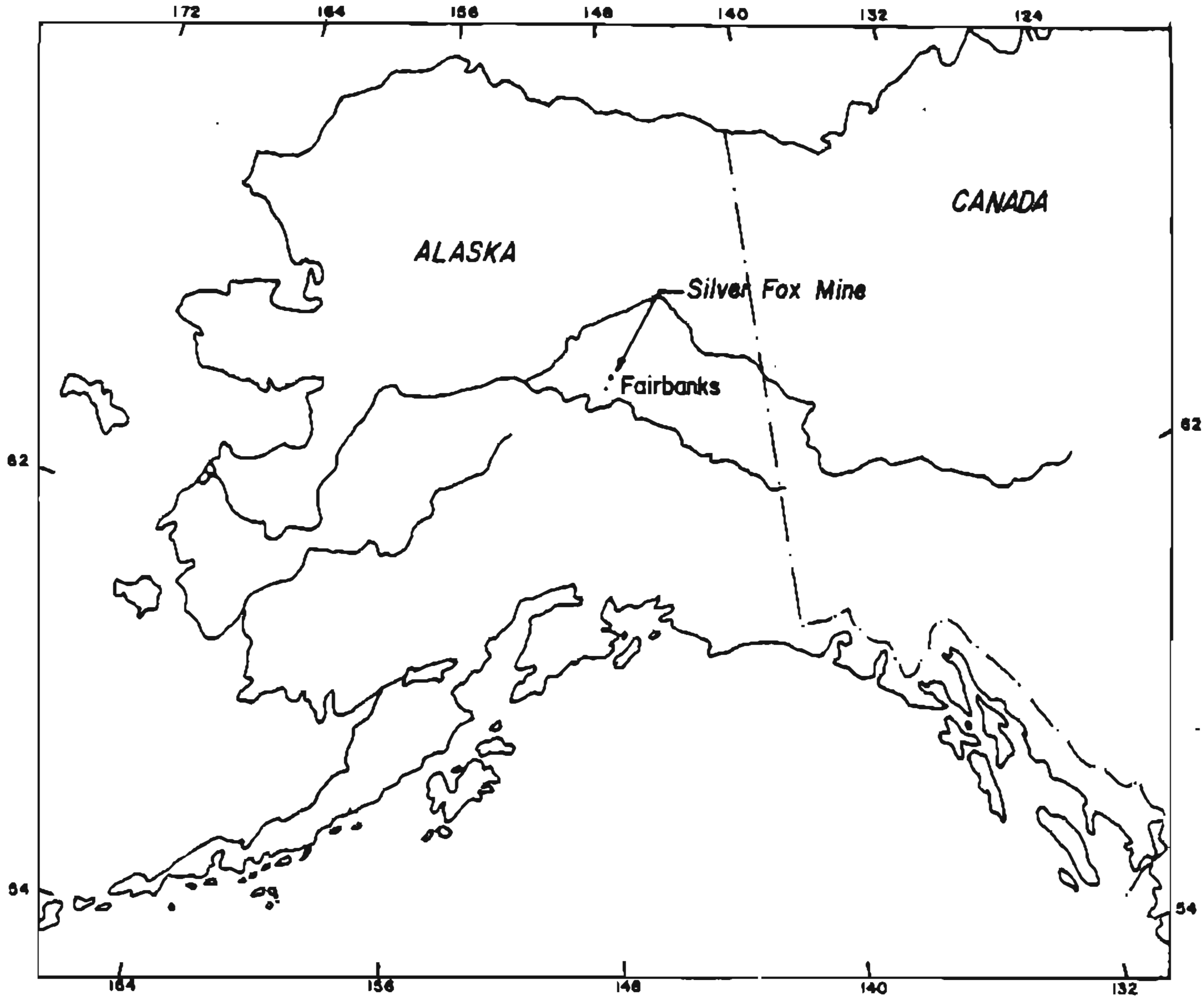

Figure 1. Location of study area, Fairbanks mining district, Alaska.

Exposure is notably poor in areas where no excavations exist;, hence, much geologic information on plate 1 is based on float and rubble crop and should be considered interpretive.

Previous Work

The Fairbanks mining district has been examined by many authors, notably Prindle and others (1913), Hill (1933), Forbes and Brown (1961), Brown (1962), Forbes and others (1968), Mowatt (1974), Britton (1968), Forbes (1982), and Forbes and Weber (1982).

Some authors briefly examined the Silver Fox property in the course of broader regional studies. Britton's (1969) study of the intrusive rocks of the Pedro Dome area provided a petrographic background of the rocks in the Silver Fox Mine area. Various government agencies have also visited the property, but most of that information has not been published. Mowatt (1974) provided the most detailed description of the mineralization of the property prior to this study.

Method of Study

Rock samples were collected for thin section to study alteration assemblages, and polished sections of the galena-sphalerite-pyrite veins were analyzed to determine paragenesis. Chip and grab samples of vein and wallrock material and soil samples taken over a regular grid were analyzed for several trace elements. A magnetometer survey was conducted over the same grid to define any distinct geomagnetic signatures.

Acknowledgments

This study was funded in part by fellowships from the U.S. Department of Health, Education, and Welfare (now Health and Human Services) and the University of Alaska (Fairbanks) School of Mineral Industry.

I wish to thank my graduate committee, particularly T.E. Smith for his continued assistance throughout the project and for his thoughtful review of the manuscript. Special thanks are due Tury Anderson, former owner of the Silver Fox Mine, for sharing his knowledge of the area. Lastly, I would like to thank my wife, Vicki, for her continued support both in the field and otherwise.

GEOLOGIC SETTING

Regional Geology

The main rock unit throughout the Fairbanks mining district is the Birch Creek schist, also called the Yukon-Tanana metamorphic complex (Foster and others, 1973). Within the area of interest, the Birch Creek schist can be divided into two broad groups consisting of a greenschist facies and an epidote-amphibolite facies.

The greenschist facies is more common and consists of micaceous quartzite, garnet-mica schist, quartz-mica schist, and phyllitic schist with subordinate greenschist and rare, impure tremolitic marble. Metamorphic grade decreases to the northwest. The epidote-amphibolite facies consists of calc-silicate marble, eclogitic rock, garnet amphibolite, epidote amphibolite, garnet-mica schist, and graphitic and micaceous quartzite. These rocks are exposed along a band from Dome Creek through Juniper Creek to the east. The epidote-amphibolite facies rocks are in low angle thrust(?) contact with the greenschist facies to the southeast (fig. 2).

Recent work by DGGS and the Mineral Industry Research Laboratory, University of Alaska, Fairbanks, has resulted in subdivision of the

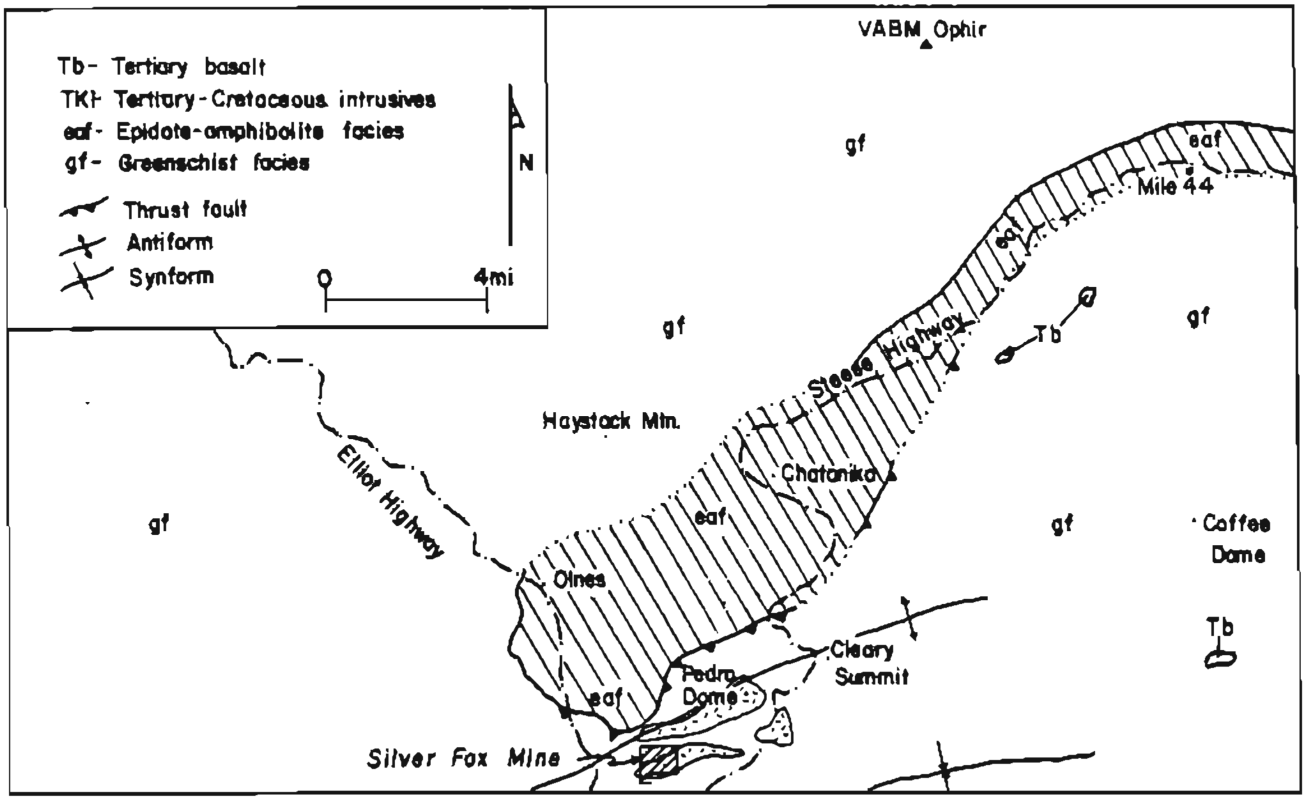

Figure 2. Geologic sketch map of a portion of the Fairbanks mining district, Alaska.

metamorphic rocks into three groups consisting of a) the Fairbanks schist terrane comprised of micaceous schists and quartzites, b) the Goldstream terrane that consists of amphibolites and pelitic schist, and c) an eclogitic sequence that contains the rocks described previously under the epidote-amphibolite facies.

Within the Fairbanks schist terrane, a distal volcanogenic package consisting of white felsic schist, graphite schist, and marble has been recognized and named the Cleary sequence. This sequence plays a major role in the distribution of gold-stibnite mineralization in the district. The rocks are generally exposed on northeast-trending antiforms in the district. They are present in the Silver Fox Mine area, along the Cleary antiform.

Metamorphic rocks in the Fairbanks mining district have undergone two periods of deformation; the first produced small-scale isoclinal recumbent folds that trend northwest, and the second produced long-wavelength folds with northeast-trending axes. Igneous rocks of the Silver Fox Mine are localized along the Cleary antiform, a product of the second fold event.

Intrusive rocks in the Fairbanks mining district range in composition from granite to quartz diorite. Igneous rocks in the Livengood Quadrangle are Cretaceous in age (Chapman and others, 1971). Quartz diorite-granodiorite intrusives in the Pedro Dome area have been dated at 90.7 ± 5.1 million years, while the quartz monzonites are 93 ± 5 million years old (Britton, 1969).

Minor volcanic rocks, specifically olivine basalts, are present near Fairbanks Creek, Alder Creek, and Kokomo Creek (fig. 2).

Metamorphic Rocks

Metamorphic rocks in the area of the Silver Fox Mine consist primarily of quartz-muscovite and muscovite-quartz schist. Minor quartz-biotite hornfels occur in contact zones of the intrusive rocks. Because no contacts with the Birch Creek schist were observed, the width of the contact aureole is unknown.

Mineralized intrusives of the mine occupy the southern flank of the Cleary antiform (pl. 1). No mineralization was found in the metamorphic rocks of the Silver Fox Mine except for some minor quartz veins (with stibnite lenses) with gold values from 0.3 to 20 ppm (Forbes and others, 1968).

Intrusive Rocks

The petrography of the intrusive rocks of the Pedro Dome area is described by Britton (1969). In this study, thin sections were examined primarily to gain an understanding of the hydrothermal alteration associated with the mineralizing process.

Quartz Diorite

The quartz diorite stock, which trends roughly east-west, makes up the largest mass of intrusive rock on the property (pl. 1). It hosts most of the mineralization, including galena-sphalerite-pyrite fissure veins and a molybdenum-bearing quartz-stockwork system.

The quartz diorite is typically fine-grained and equigranular; plagioclase is the most abundant mineral. Quartz is anhedral to subhedral or occurs as micrographic intergrowths with potassium feldspar. Biotite is more common than hornblende and is often seen as a secondary rim around the latter. Accessory minerals include apatite, sphene, epidote, and magnetite.

A granodiorite variant of the quartz diorite (sample 14-19, pl. 1) has a porphyritic texture with quartz and zoned plagioclase as phenocrysts. The matrix consists of quartz, plagioclase, and micrographic intergrowths of potassium feldspar.

Jointing within the quartz diorite is common and at least two distinct sets were noted. Figure 3 is a contour diagram of a lower-hemisphere plot of the poles of 157 joints and faults. Note that the most common orientation is a northeasterly set that dips southeast and a northwesterly set that dips northeast. These may represent a conjugate set of fractures and faults that formed during the cooling of the stock after intrusion. Faulting is common within the quartz diorite, although displacements tend to be less than 1 ft.

A stockwork vein system composed of quartz ± molybdenite, calcite, scheelite, and zeolites is exposed underground in the quartz diorite. The density of the stockwork fracture system varies, but it is more fully developed in the westernmost part of the workings. Surface exposures of the stockwork system are generally lacking.

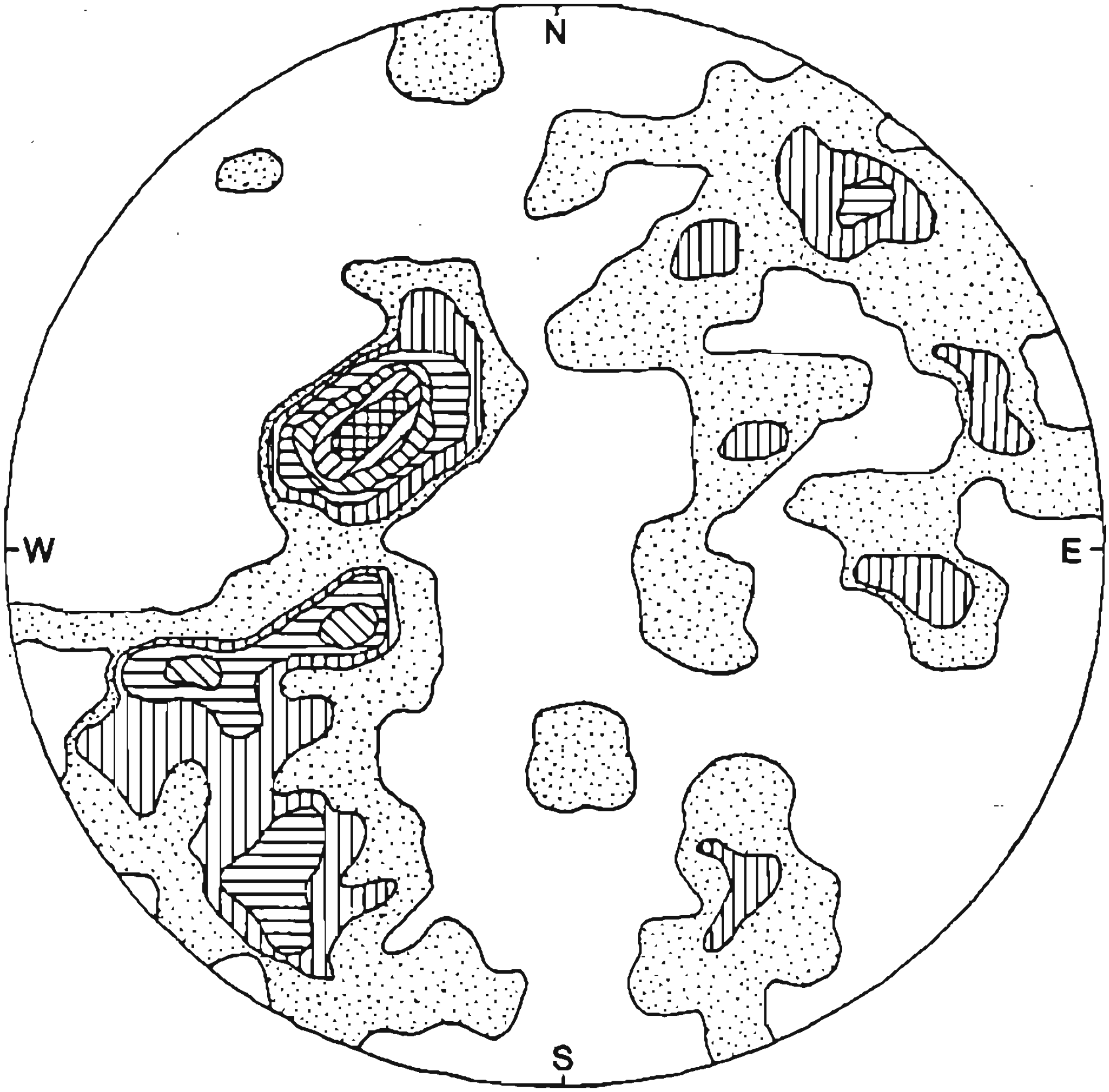

Figure 3. Contour diagram of poles of joints and faults; base contour and contour interval is 1 percent.

Quartz monzonite

Two bodies of quartz monzonite are present on the property (pl. 1). Because the eastern stock is poorly exposed, the location of the eastern contact with the Birch Creek schist is unknown. The western body is better delineated because of the large number of excavations in the immediate area. Britton (1969) named these stocks the Flume and Fox Creek plutons, respectively. Although similar in appearance, there are significant differences between the plutons.

Two textural variations were noted in the Flume Creek pluton, but their contact relations were not established because of poor exposure. One variant is a coarse, equigranular quartz monzonite dominated by potassium feldspar. The other variant is a fine-grained, porphyritic quartz monzonite of similar bulk composition that may represent a dike or contact zone rather than a different phase of the main intrusive.

The Fox Creek pluton is composed of coarse-grained, nearly equigranular quartz monzonite, whose margins are cut by numerous dikes. Roof pendants of hornfelsed schist are common, which indicates that the upper portion or hood zone of the intrusive is presently exposed (fig. 4). Large quartz veins are present in the stock; the attendant alteration will be discussed later. Because much of the stock is highly altered, structural relationships are obscured. Appendix A lists modal analyses of the intrusive rocks.

Intrusive Relationships

Field evidence suggests the quartz diorite was emplaced before the quartz monzonite, which may have been intruded into zones of weakness along the contacts (Britton, 1969). One xenolith of quartz diorite was found in the quartz monzonite of the Flume Creek pluton. No dikes of quartz monzonite appear to crosscut the quartz diorite; instead, the contact consists of relatively fresh quartz monzonite adjacent to grus from the weathered quartz diorite.

According to Britton (1969), quartz monzonite dikes cut quartz diorite in a road cut along the Twin Creek pluton. If the intrusives in the Pedro Dome region have a common genetic origin, this would also confirm the intrusive sequence suggested for the Silver Fox Mine.

ALTERATION AND MINERALIZATION

Characteristic Alteration Types

The intrusive rocks exhibit potassic, sericitic, argillic, and propylitic alteration. Potassic alteration is typically represented by potassium-feldspar veinlets or flooding and is generally restricted to the quartz diorite, although it is present in two locations within the Fox Creek pluton. Some potassium-feldspar veinlets display distinct envelopes of sericite and chloritized biotite.

Pervasive sericitization is present at several locations within the Flume Creek pluton. Typically, this alteration ranges from minor dusting of the plagioclase to near total destruction of the original minerals (fig. 5).

Kaolinite is found in nearly all samples but is rarely pervasive. Such clay alteration is generally more common in the quartz monzonite. In the Fox Creek pluton, the large quantities of clay that are present are apparently related to large, often obscured, quartz veins such as those shown in figure 6. Much of the argillic alteration is confined to calcic cores of plagioclase grains, and may be supergene in origin.

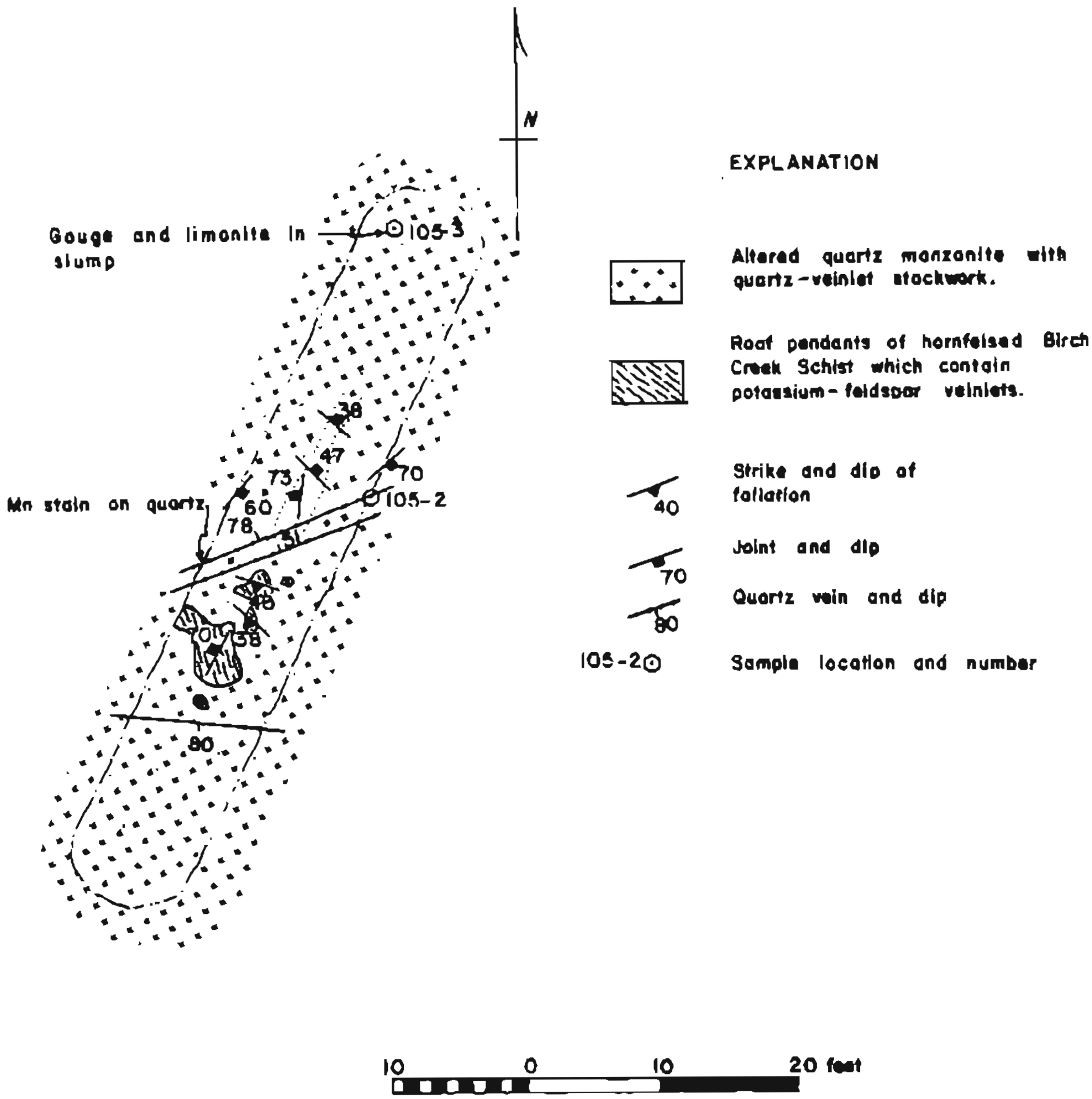

Figure 4. Map of trench in the Fox Creek pluton; note roof pendants of hornfelsed schist (loc. 1, pl. 1).

Propylitic alteration is best observed in the underground workings in the quartz diorite, where biotite has been altered to chlorite and minor epidote. Calcite veinlets are common and typically cut the quartz-molybdenite stockwork. Crosscutting and offsetting of calcite veinlets indicates two generations of calcite. Large carbonate lenses and pods that are often present within the quartz diorite contain some pyrite along the contact with the host rock. The propylitic alteration imparts a marked greenish cast to quartz diorite in the underground workings. Because the quartz monzonite has scant mafic minerals, the effect of propylitic alteration is not very pronounced, although minor calcite is present.

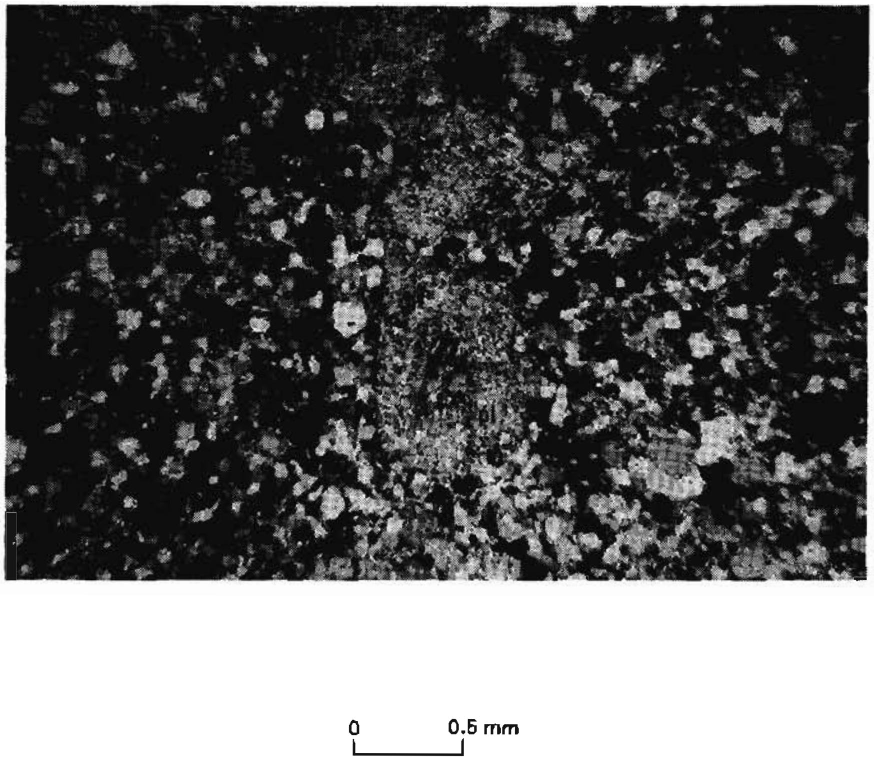

Figure 5. Photomicrograph of sericitic alteration of plagioclase, Flume Creek pluton, Fairbanks mining district, Alaska.

Figure 7 is an alteration map of the study area. Contacts are based on samples collected from the few available exposures and are therefore considered approximate. The area of potassic alteration appears to be confined primarily to the quartz diorite; however, potassium-feldspar-bearing veinlets do occur within the quartz monzonite in the contact area of a roof pendant (fig. 4) and as small grains in a quartz veinlet (sample 46-6, pl. 1). The contact of the sericitic zone is based on samples that show pervasive alteration. While the sericitic zone appears to overlap the potassic zone, actual evidence of overprinting was not observed. Although the alteration map is based on few samples, it does provide an approximate areal distribution of the assemblages.

Feldspar in both quartz monzonite bodies often shows considerable argillization. This has been related to veinlet control in only a few cases. Much of the argillic alteration in the quartz monzonite may be of supergene origin, excluding the obvious hypogene alteration that accompanies the large quartz veins in the Fox Creek pluton.

Sulfide Veins

Sulfide veins were the major target at the time of initial discovery and development of the property. Galena in the veins is argentiferous, and early reports indicated assays of 168 ounces per ton (Anonymous, 1913). However, analyses of samples in this study revealed values considerably lower. Table 1 lists the analyses of several grab and chip samples from various fresh and oxidized veins (locations shown on pl. 1).

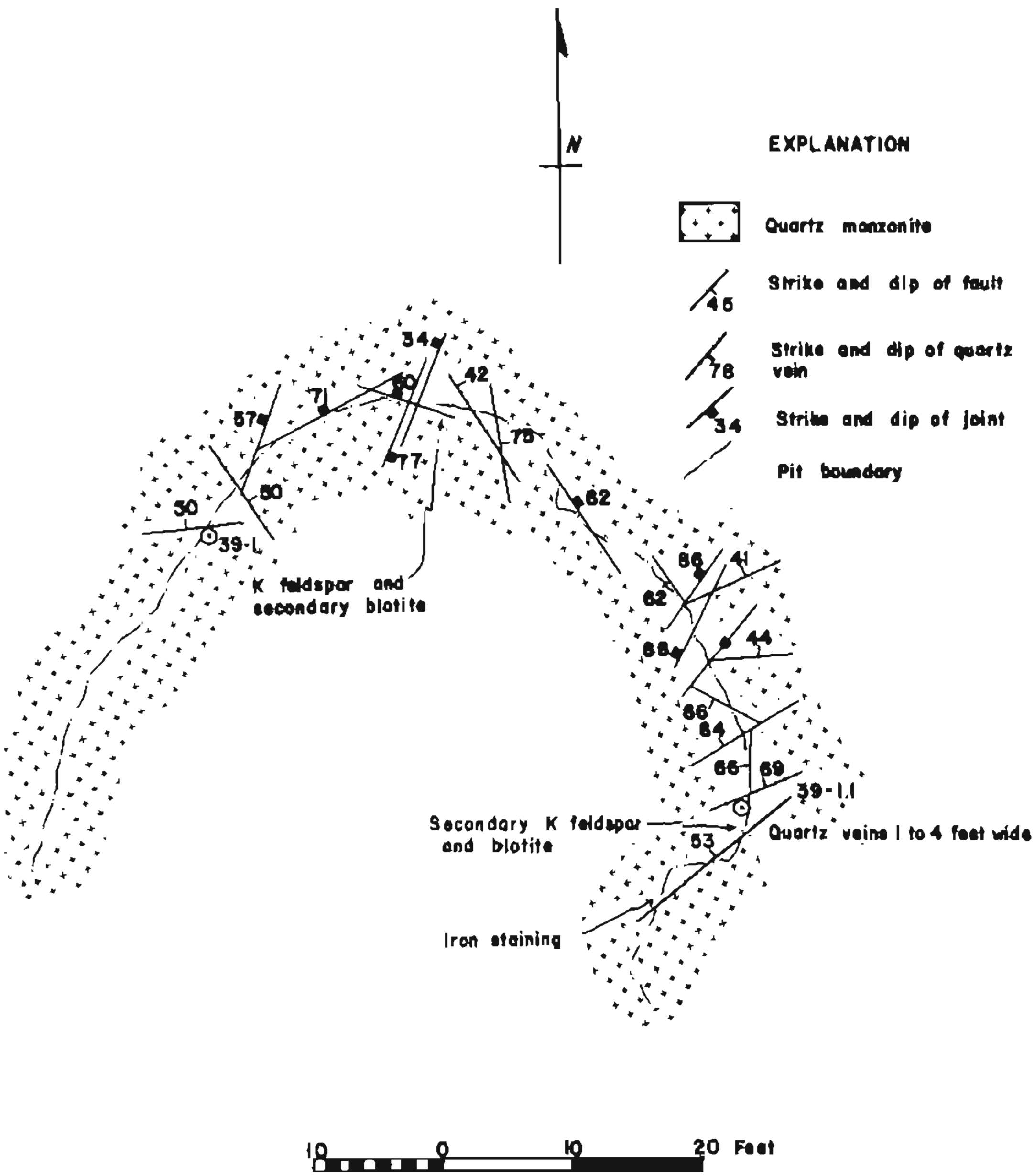

Figure 6. Pit map showing quartz veins and the associated potassium-feldspar and biotite in the Fox Creek pluton (loc. 2, pl. 1), Fairbanks mining district, Alaska.

Argentiferous galena, sphalerite, pyrite ± chalcopyrite, and arsenopyrite are present in the veins. In polished section, chalcopyrite is present as emulsion exsolutions (fig. 8) within the sphalerite, which may indicate a minimum temperature of formation of 350°C. Much of the sphalerite does not contain chalcopyrite, which suggests that deposition of sphalerite continued after initial deposition of the sulfide. Pyrite and arsenopyrite are highly

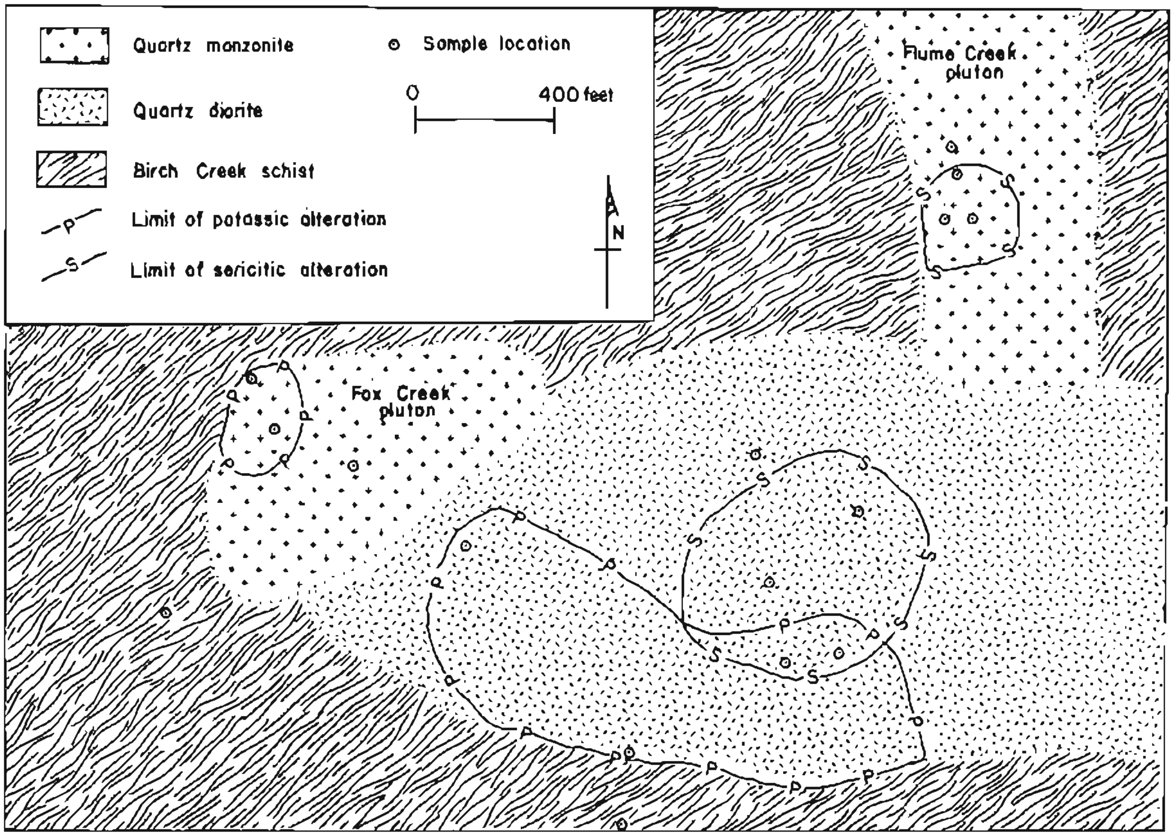

Figure 7. Alteration map of a portion of the study area, Silver Fox Mine, Fairbanks mining district, Alaska.

fractured, and later calcite fills the voids. Figure 9 shows the envisioned paragenetic sequence within the fissure veins. Anglesite and limonite are common in the secondary environment. Calcite is the major gangue mineral in the underground veins, but veins on the surface are oxidized and any original calcite has been leached by acids produced from weathering pyrite. The veins are typically irregular, narrow, discontinuous features that were deposited along joints and in some cases, shear zones. The widest underground vein reaches a maximum width of 18 in. in some places.

No obvious vertical zoning pattern can be distinguished, although it does appear that gold and silver are more concentrated in the near-surface veins. This may be caused by relative enrichment of gold and silver in the secondary environment. Lead and zinc are present in smaller quantities in the surface veins versus the underground vein, which reflects the effect of base-metal leaching on the surface.

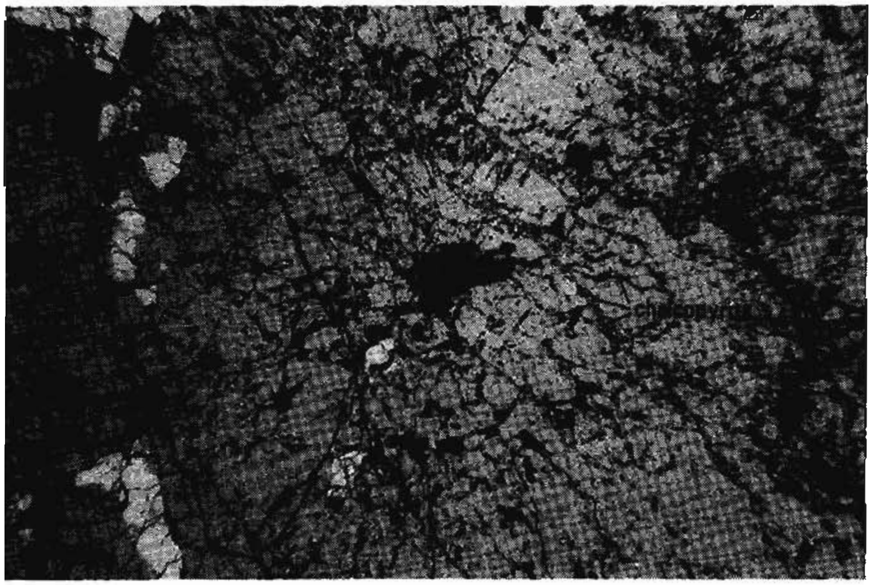

Figure 8. Photomicrograph of chalcopyrite exsolution blebs in sphalerite, Silver Fox Mine, Fairbanks mining district, Alaska.

	------------------------TIME-----------------------
pyrite	---------- ?-----?
arsenopyrite	----------
chalcopyrite	----------
sphalerite	----------?-----?
galena	---------
calcite	?---?---?---?---?---?-----------------

Figure 9. Paragenetic sequence of sulfide veins in the quartz diorite. Extensive fracturing occurred after deposition of the pyrite and arsenopyrite, and minor fracturing may have occurred after deposition of the sphalerite and chalcopyrite; Silver Fox Mine, Fairbanks mining district, Alaska.

Table 1. Atomic-absorption analyses of grab and chip samples from sulfide veins in the quartz diorite; all values in ppm.

Sample no.	Sample type	Cu	Pb	Zn	Mo	Au	Ag
36-1	Grab	680	9900	1160	8	70.0	975
36-2	Grab	36	8900	2100	4	11.7	663
60-1	Chip	100	7700	19400	5	-0.01	79
60-2	Chip	100	7700	19400	5	-0.1	79
70-2	Grab	4000	9000	800	19	2.9	1120
107-1	Chip	149	29600	1600	35	0.8	92
107-4	Grab	760	95500	37600	6	1.4	662

The mineralized veins appear to be restricted to the quartz diorite body because none have been found within the quartz monzonite intrusives or the Birch Creek schist. The absence of sulfide veins in the schists may be due to the failure of the micaceous rocks to form dilatant zones. The sulfide-vein mineralization appears to be related to the intrusion of the quartz diorite, because similar mineralization is absent in the younger quartz monzonite.

Most faulting involves small displacements, and has offset almost all of the veins. Figure 10 is a map of a pit excavated during surface mining of three subparallel veins. The veins have been blocked out by faulting along a northeast-trending shear zone to the west and a strike-slip fault to the east. The extension of these veins has not been located on either side of the faults. Other similar cases occur throughout the area. Figure 11 is a map of another mineralized pit in which the mineralization is discontinuous along strike. Actual vein and fault relationships are not well exposed, except for those in figure 10. Trenching along strike has, in most instances, not revealed the extension of faulted veins.

Figure 12 is a plot of the poles of 157 joints and faults and includes the attitudes of the sulfide veins. Seventy-five percent of the veins strike north-northwest to east-west and dip south-southwest. Dips vary from steep to moderately shallow. This loose grouping of veins shows a preferential orientation and indicates which fissures were dilatant during ore deposition.

The vein exposed underground occupies a shear zone and is pinched out near the end of the drift (pl. 2). This is the only vein exposed thus far underground, and actual mineable tonnages are probably small. Attempts to locate the extension of the vein by drilling at the point of pinchout have failed. A short inclined winze also failed to reveal additional mineralization.

Alteration around the sulfide veins appears to follow the pattern described by Meyer and Hemley (1967) for veins in granodioritic host rocks. A sericitic envelope, often with disseminated pyrite, is located closest to the vein; an argillic alteration envelope is adjacent to it. Such envelopes are not very large, and where observed on the surface are less than 18 in. wide. Disseminated pyrite was reportedly encountered underground prior to actual intersection of the vein, and its presence may provide an indicator of nearby vein mineralization.

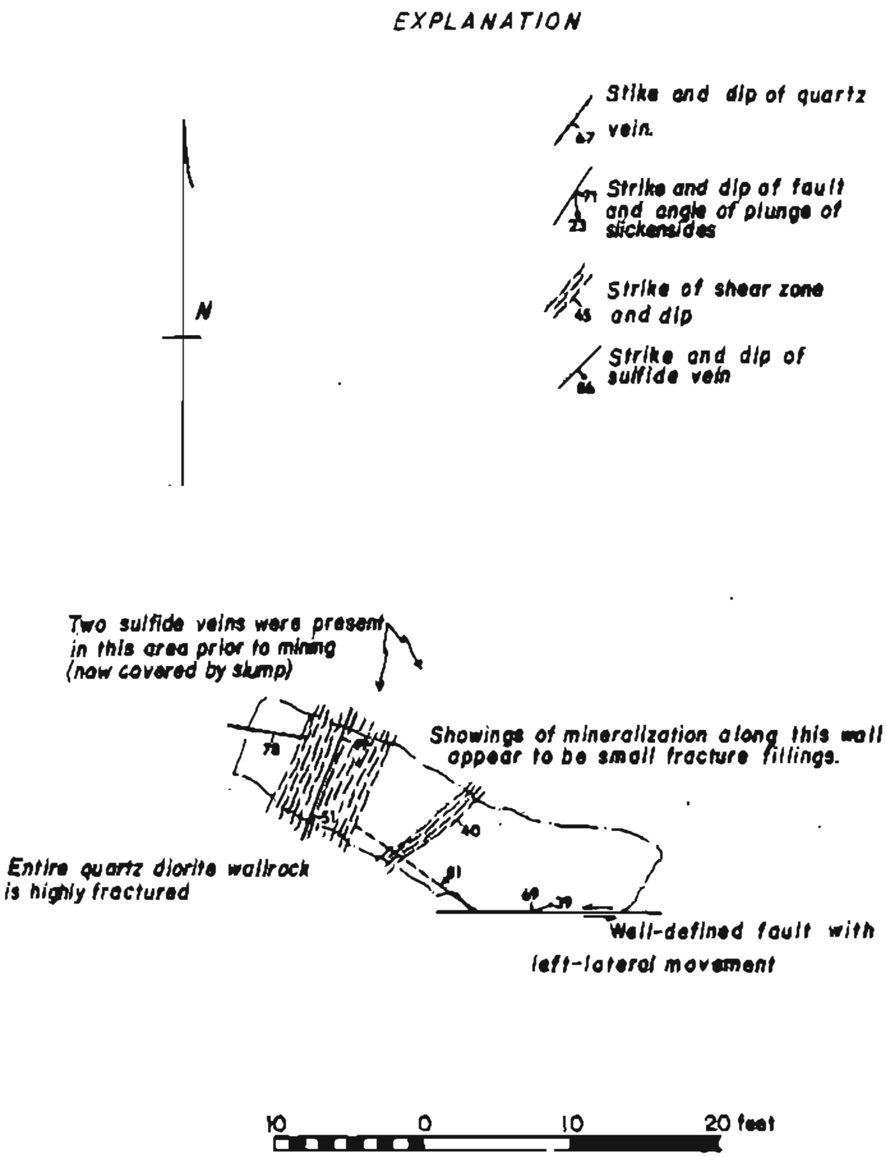

Figure 10. Pit map of an area in the quartz diorite where three parallel veins existed prior to mining (loc. 3, pl. 1), Silver Fox Mine, Fairbanks mining district, Alaska.

Quartz Stockwork in the Quartz Diorite

A variable density stockwork-vein system is exposed in the underground workings of the mine. The presence of molybdenum in this system was first reported by Mowatt (1974). Molybdenite occurs as disseminated crystals up to 3/8 in. in diameter and as smeared coatings along contacts between the quartz stockwork and wallrock. No molybdenite was observed on the east side of the mineralized shear in the westernmost drift of the mine (pl. 2). This may represent a faulted block because, as recognized by Mowatt (1974), fracturing

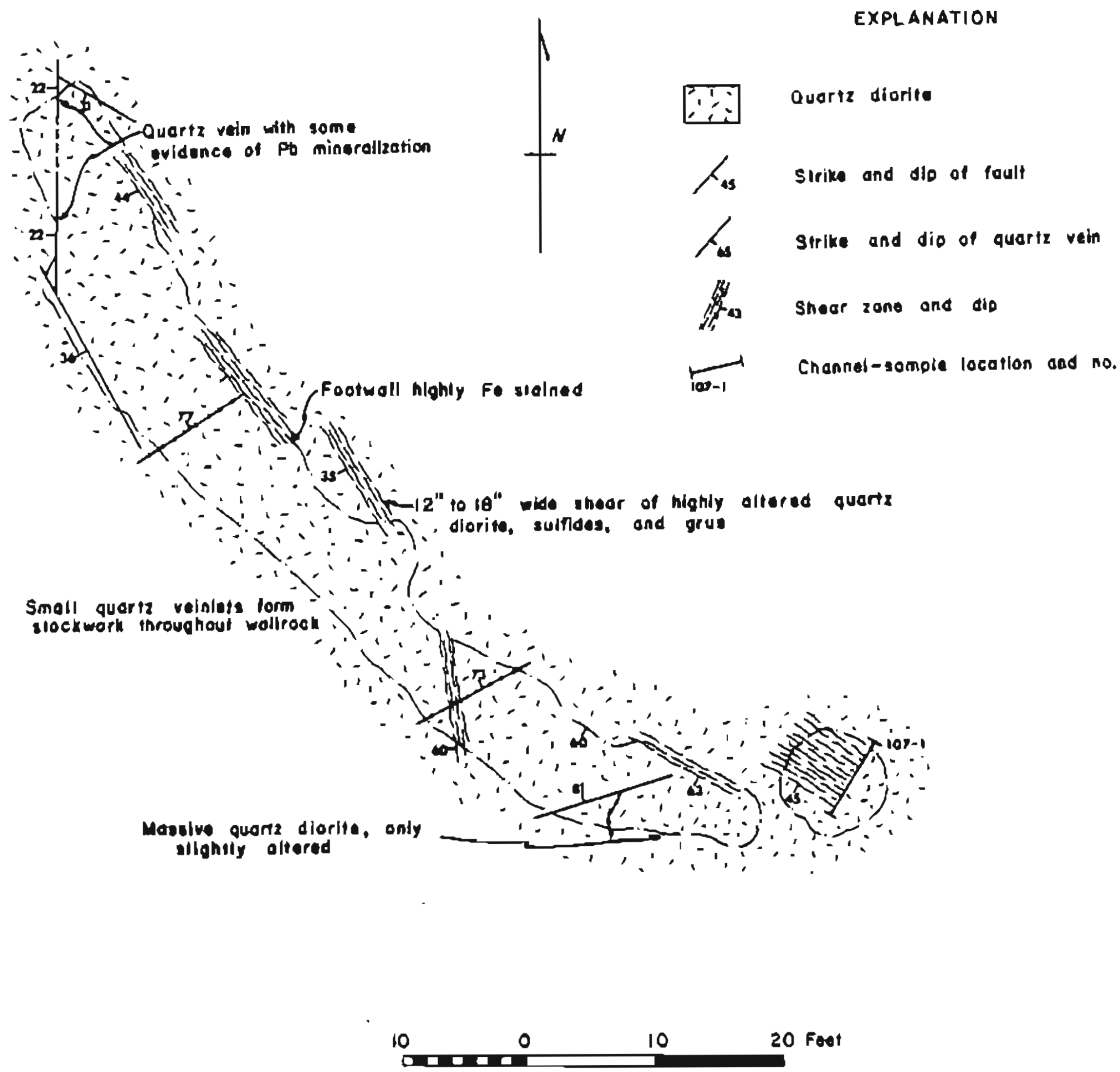

Figure 11. Pit map of a sulfide-bearing shear zone in the quartz diorite; extension of shear beyond pit has not been located (loc. 4, pl. 1); Silver Fox Mine, Fairbanks mining district, Alaska.

and intensity of the stockwork increases west of the shear zone. No quantitative estimation of displacement can be made because of lack of visible offset features. The absence of molybdenite east of the shear and the change in the stockwork character seem to indicate that a 'deeper' portion of the intrusive system has been exposed.

The mineralogy of the quartz stockwork is simple, consisting of quartz, molybdenite, scheelite and ± potassium-feldspar. Pyrite occurs irregularly within the wallrock, and makes up as much as 15 percent of the total rock composition in several cases.

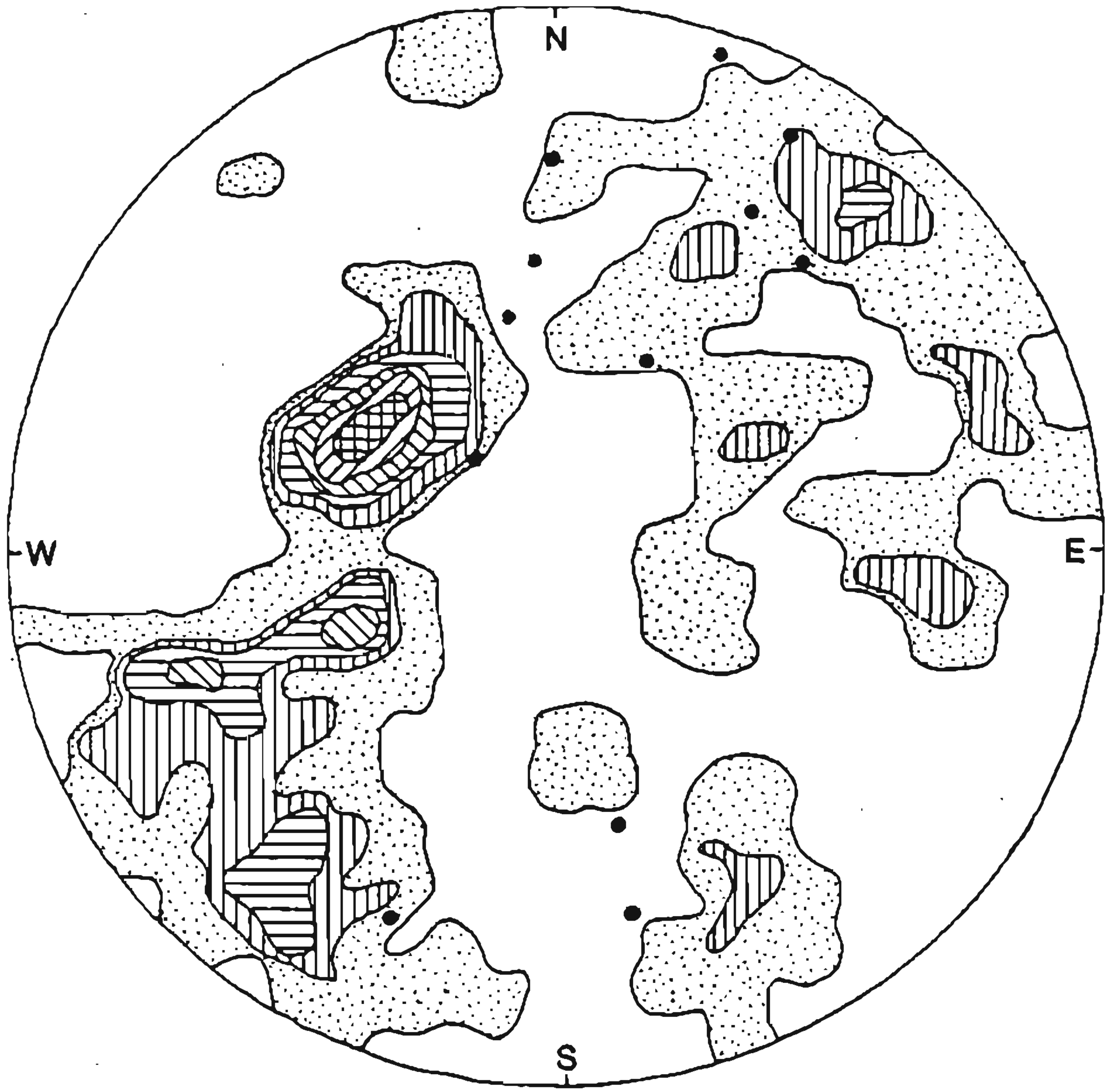

Figure 12. Contour diagram of poles of joints and faults. Circles show attitude of sulfide veins. Base contour and contour interval is 1 percent. Silver Fox Mine, Fairbanks mining district, Alaska.

Potassic alteration is present within the stockwork and occurs as veinlets cross-cutting the quartz veins and as very minor veinlets along the periphery of the quartz veins. Fracturing of the quartz after initial deposition prepared the way for the introduction of at least two generations of calcite veinlets. Figure 13 shows the general relationship between the stockwork and the subsequent calcite phase, which also contains minor pyrite and chalcopyrite. The potassium-feldspar phase also occupies portions of these fractures. Table 2 lists analyses from the underground stockwork. Molybdenum and tungsten occur in very small amounts within the chip sample of the face. Although large blebs and surface coatings of molybdenite are present, they do not approach the economic grades of 1,500 to 5,000 ppm common in other molybdenum-producing stockworks.

Molybdenum was found at only one location on the surface, and no other occurrences are known. Sample 38-2 (pl. 1) contains molybdenite, chalcopyrite, and pyrite associated with narrow ($<$ 3mm) quartz veinlets.

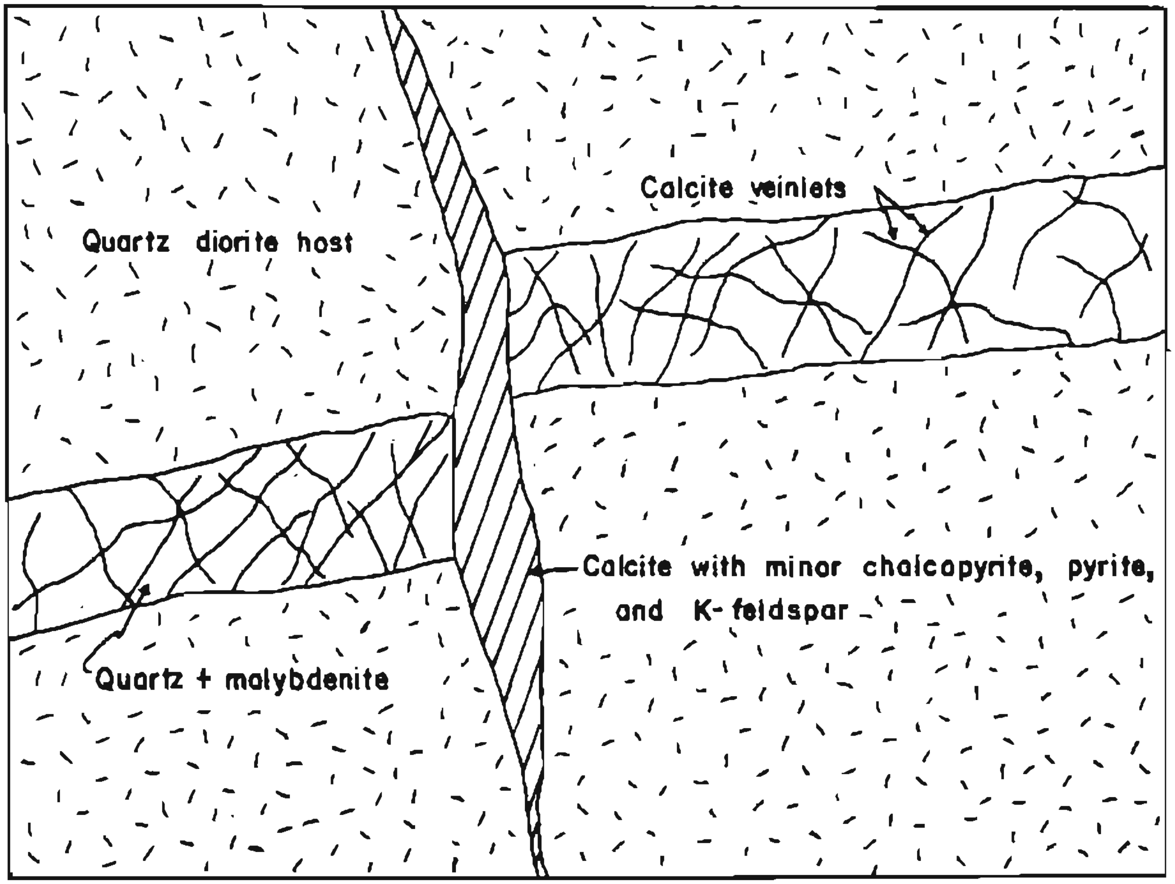

Figure 13. General characteristics of the quartz-molybednite stockwork exposed underground, Silver Fox Mine, Fairbanks mining district, Alaska.

Table 2. Atomic-absorption analyses of samples from the underground quartz-molybdenite stockwork; all values in ppm.

Sample no.	Sample type	Cu	Pb	Zn	Mo	Au	Ag	W
60-3	Grab	14	146	81	11	-0.1	2	-
60-4	Grab	13	490	93	9	-0.1	1	-
107-3	Chip	9	-	-	8	-	-	35

- No analysis requested

The surface in the area of this sample is moderately iron-stained, and in thin section limonite is pervasive, which suggests that pyrite was present prior to weathering. Because trenching in this area did not reveal further mineralization, the relationship of this occurrence to underground exposures is uncertain. The chalcopyrite grains in this sample are 2 to 3 mm in size, which contrasts sharply with the underground stockwork in which megascopic chalcopyrite is virtually absent. A geochemical analysis of this sample yielded 1,900 ppm copper, 1,040 ppm lead, and 120 ppm molybdenum (sample 38-2, app. B). No lead minerals were observed in the grab sample.

The genesis of this stockwork appears to be related to early cooling after initial emplacement of the pluton. In this model, residual magmatic fluids carrying silica, molybdenum, and tungsten entered tension cracks formed by the cooling process. Molybdenite deposited along the walls of the quartz veins was sheared and smeared during subsequent movement along the veins.

Quartz Veins in the Quartz Monzonite

The quartz monzonite bodies are cut by quartz veins of varying size. The Flume Creek pluton contains only small ($<$2mm) quartz veinlets, while the Fox Creek pluton contains quartz veins approaching 2 ft in width. Alteration associated with these large quartz veins consists primarily of argillization of the wallrock. In some areas, this alteration is so intense that the entire region consists of kaolinite.

Mineralization in these areas is weakly developed, and commonly consists of gold and stibnite. Gold concentrations from analyses in this study were low. Table 3 lists analyses from quartz veins in the Fox Creek pluton. Analysis of these veins (samples 39-1 and 39-1.1, pl. 1) for gold revealed values ranging from 0.3 to 0.5 ppm. Sample 105-2 (fig. 4) contains only 5 ppb, thus indicating the gold content of the exposed quartz veins in the quartz monzonite is low. Local stibnite-bearing lenses and pods within the contact zone contain up to 27 ppm gold (Forbes and others, 1968). Stibnite is apparently the only sulfide common in the quartz monzonite; no galena or pyrite were found in any of the veins.

Although excavations in the Flume Creek pluton are few, there appears to be no mineralization in the stock.

Table 3. Atomic-absorption analyses of quartz veins from the Fox Creek pluton; all values in ppm.

Sample no.	Sample type	Cu	Pb	Zn	Mo	Au	Ag
39-1	Grab	460	7900	152	170	0.5	49
39-1.1	Grab	33	620	210	45	0.3	4
105-2	Chip	4	60	9	4	0.005	0.2
105-3	Gouge	21	68	39	43	0.015	0.2

A geochemical survey revealed a molybdenum anomaly over the Birch Creek schist near the contact with the Fox Creek pluton. The significance of this anomaly is discussed in a later section.

Excavations within the quartz monzonite are less numerous than those in the quartz diorite, and thus it is difficult to accurately assess the potential of these areas. On the basis of areas that are exposed, it appears that the quartz monzonite is more weakly mineralized, even though it has been modified by hydrothermal activity.

PROPOSED SEQUENCE OF HYDROTHERMAL EVENTS

A model (based on field and laboratory evidence) of the various magmatic and hydrothermal events is shown on plate 3. The inferred sequence is:

Stage 1: Initial emplacement of the quartz diorite-granodiorite stock. The more mafic variant is the common rock type at the Silver Fox Mine.

Stage 2: Initial cooling of the intrusion with attendant development of tensional fractures caused by shrinkage.

Stage 3: Late magmatic fluids containing silica, molybdenum, ± copper, ± tungsten were introduced along the stockwork fracture system that resulted from stage 2. Molybdenite was deposited along the contacts of the stockwork and as disseminations within the quartz veins. Scheelite is present as fracture fillings and disseminations. Sericitization of the wallrock may have occurred at this time.

Stage 4: Further cooling of the intrusive and movement along the quartz-filled stockwork fractures resulted in smearing of molybdenite along the contacts. This movement also resulted in fracturing of the quartz veins.

Stage 5: A carbonate phase was introduced along dilatant fractures, replaced some quartz, and filled the small-scale fractures in the stockwork to form calcite veinlets.

Stage 6: Additional faulting resulted in the uplift of 'molybdenum-rich' stockwork against 'molybdenum-poor' stockwork.

Stage 7: Further thermal collapse of the system made the environment suitable for deposition of lead, zinc, iron, arsenic ± copper sulfides along joint planes and shear zones. This resulted in veins of argentiferous galena, sphalerite, pyrite ± chalcopyrite, and arsenopyrite. Because these veins are crosscut by calcite stringers, stages 5 and 6 may be reversed or a later calcite event occurred with ore deposition.

Stage 8: Renewed activity and differentiation at depth resulted in the formation of the late-stage quartz monzonite magma that was emplaced along the contact area of the quartz diorite.

Stage 9: Residual fluids rich in silica, alumina, and potash accumulated within the chamber.

Stage 10: A potassic-fluid phase was introduced along dilatant fractures at depth, invaded the area of the quartz-molybdenite stockwork, and entered preferential zones within the quartz monzonite. These fractures offset the quartz veins of the stockwork. In some areas, potassium-feldspar alteration of the stockwork resulted in remnant quartz cut by calcite veinlets surrounded by orthoclase laths (fig. 14). The potassium-feldspar flooding was not pervasive, and most of the original quartz stockwork was unaffected.

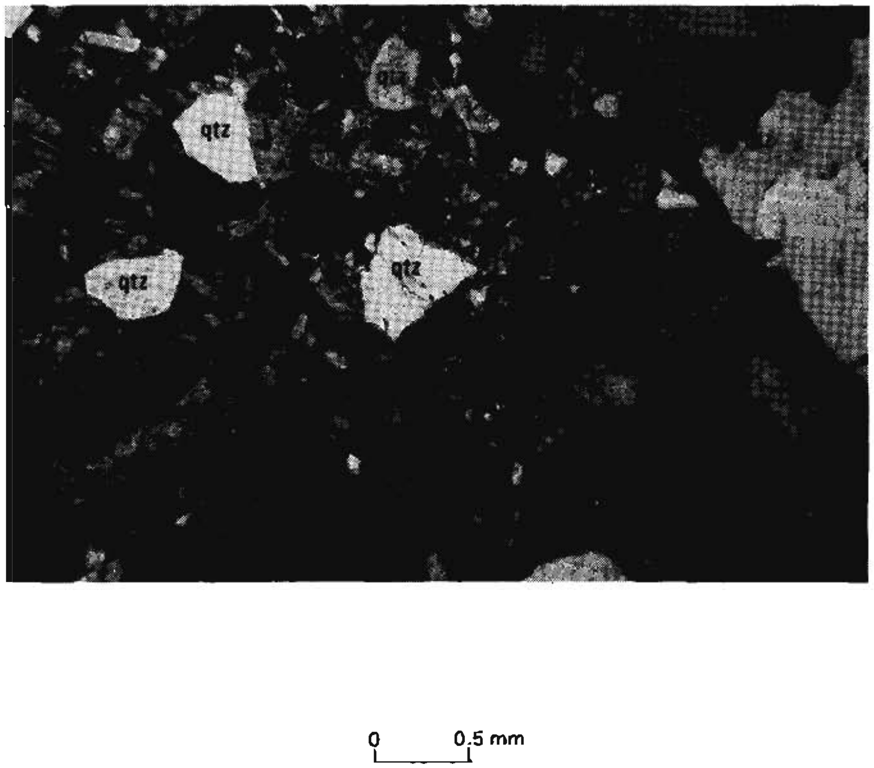

Figure 14. Photomicrograph of potassium-feldspar flooding in the quartz-molybdenum stockwork, Silver Fox Mine, Fairbanks mining district, Alaska.

Stage 11: A carbonate phase introduced along the same fractures as those noted above resulted in resorption of some of the potassium-feldspar and deposition of very minor pyrite and chalcopyrite.

Stage 12: Along the margins of the Fox Creek pluton, quartz veins with very minor gold and stibnite were deposited during the late stages. Stibnite mineralization was also introduced in portions of the contact hornfels.

Because the potassium-feldspar cuts portions of the mineralized stockwork in the quartz diorite, this sequence represents two distinct periods of hydrothermal activity. A less attractive explanation is that the potassium-feldspar alteration phase (stage 10) may have been related to the differentiation of the quartz diorite rather than the residual fluids of the quartz monzonite; there is no conclusive evidence supporting this theory.

GEOCHEMICAL SAMPLING

Introduction

A soil-sampling program was undertaken over part of the claim block to determine if any unknown mineralized areas existed. The central claim line trends N 65° W and was used as a baseline for the 3,000- by 1,600-ft grid (pl. 1). Samples were taken at 200- by 100-ft grid intersections that were located by compass and tape. Hand augers were used in an attempt to consistently sample the 'B' horizon. The -80-mesh fraction of the soil samples was analyzed for copper, lead, zinc, molybdenum, and silver by atomic absorption.

Permafrost and contamination were the two main problems encountered in the sampling program. The presence of permafrost on most north-facing slopes made sampling of the 'B' horizon difficult. At a few locations, only the upper portion of the 'A' horizon was accessible; hence, analyses for these samples may not be comparable with the rest of the survey.

Contamination from the large number of excavations on the property also presents a problem in the treatment of the data. Dispersion from open mineralized areas caused elevated values downslope. These were recognized by their proximity to mineralized areas and confirmed in one case by trenching. Appendix C contains the data used to determine threshold and contour the elemental distribution.

Samples suspected of contamination and those which were verified as such were eliminated from the data set in determining threshold values because they do not represent the true distribution of elements in the undisturbed soil.

Determination of Threshold

Proper identification of threshold is necessary to define anomalous areas and to effectively separate them from the background population. Where possible, the method of Sinclair (1976) was applied to the modified data set to define areas of interest. Cumulative probability plots were constructed to determine the nature of the individual elemental populations.

Figure 15 is a cumulative probability plot of the copper distribution plotted arithmetically. A single normal distribution accurately defines the copper population with a mean of 19.7 ppm and a standard deviation of 5.5 ppm. The line was fitted by means of a simple linear regression. In this case, some upper values are considered anomalous until proven otherwise; a threshold is established at 31 ppm using the mean plus two standard deviations (Hawkes and Webb, 1962). Four samples are considered anomalous; three others at 30 ppm should also be considered. The significance of these and other anomalous values will be discussed later.

Figure 16 is a cumulative probability plot of the lead distribution. Lead shows a bimodal distribution and yields a curve that can be partitioned into a lower background population and an upper anomalous population. Threshold is defined at the upper one percentile, in this case 38 ppm, of the lower population. This will include a few background values, but will probably contain the majority of the truly anomalous values. There are 13 values that exceed the threshold of 38 ppm and can be considered anomalous.

The zinc data appears to consist of a single lognormally distributed population (fig. 17). The mean plus two standard deviations was used to define the threshold. The six samples above 77 ppm are considered anomalous; of these, two are associated with anomalous lead values.

The molybdenum population presents a problem in determining threshold by cumulative probability plots because 62.5 percent of all values are less than or equal to the detection limit of 1 ppm. Figure 18 is a log-cumulative probability plot of the molybdenum data. The curve has the appearance of a bimodal population consisting of 7 percent of an upper population and 92

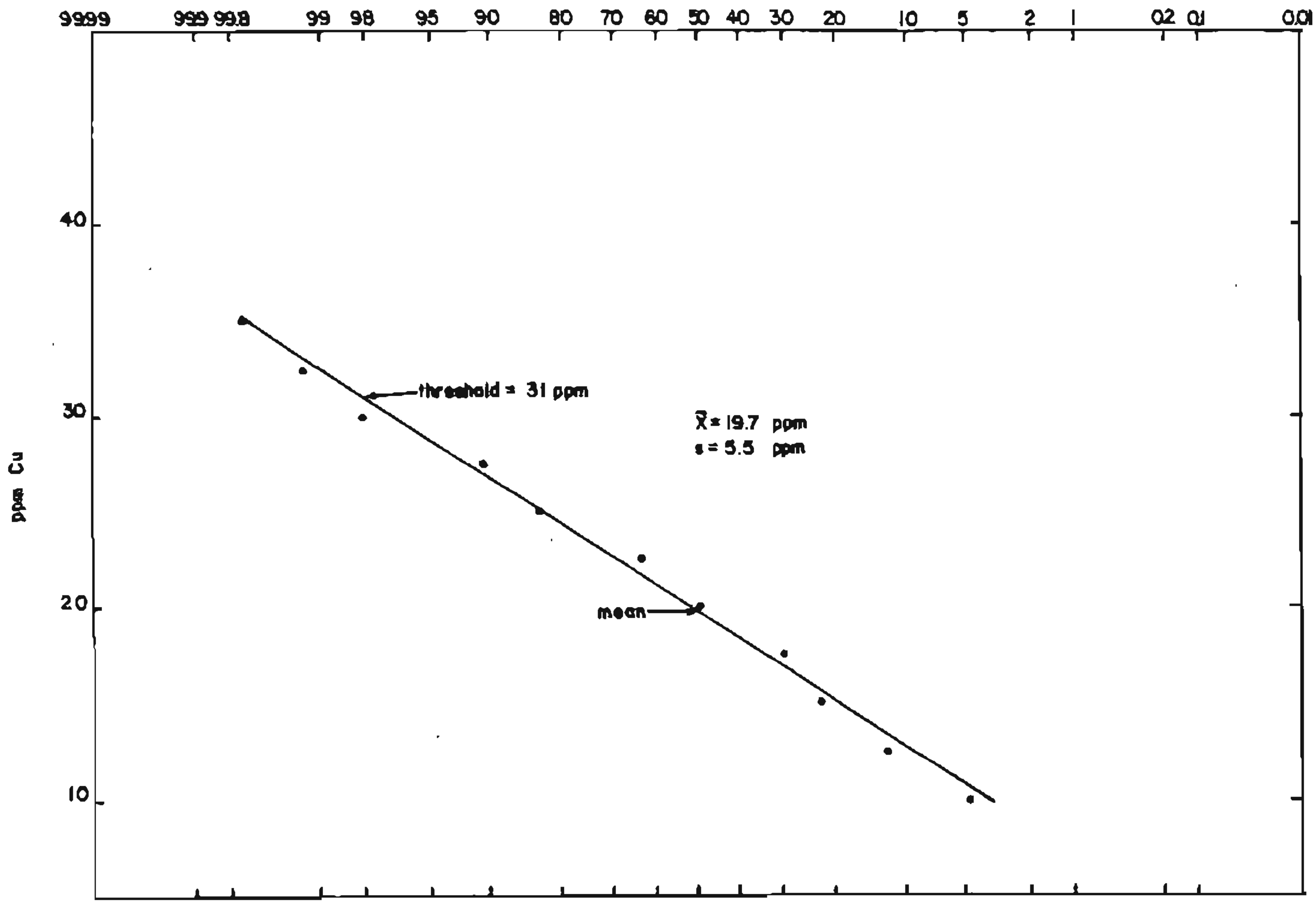

Figure 15. Cumulative probability plot of copper distribution, Silver Fox Mine, Fairbanks mining district, Alaska.

percent of a lower population. Actually, three populations exist: a) an upper anomalous, b) a lower background, and c) a truncated background population that is below the detection limit. Although the curve in figure 18 is defined by only eight points, partitioning appears feasible. Taking the upper one percentile of the lower population yields a 4 ppm threshold. Thus defined, 32 samples are anomalous in molybdenum.

In the case of the silver distribution, not much can be said because 96 percent of the values fall at or below the detection limit of 0.2 ppm. In this case, anything above 0.2 ppm is considered anomalous because it represents only 9.5 percent of the total population. This results in 23 anomalous samples.

Significance of Anomalous Values

In discussing the anomalies recognized during the study, the grid lines that run N 65° W have been designated as 'E,' and the lines that run N 25° E have been labeled 'N' for reference only.

Figure 19 is a contour map of the copper distribution showing the geology and topography. A base contour of 25 ppm was chosen; the contour interval is 5 ppm.

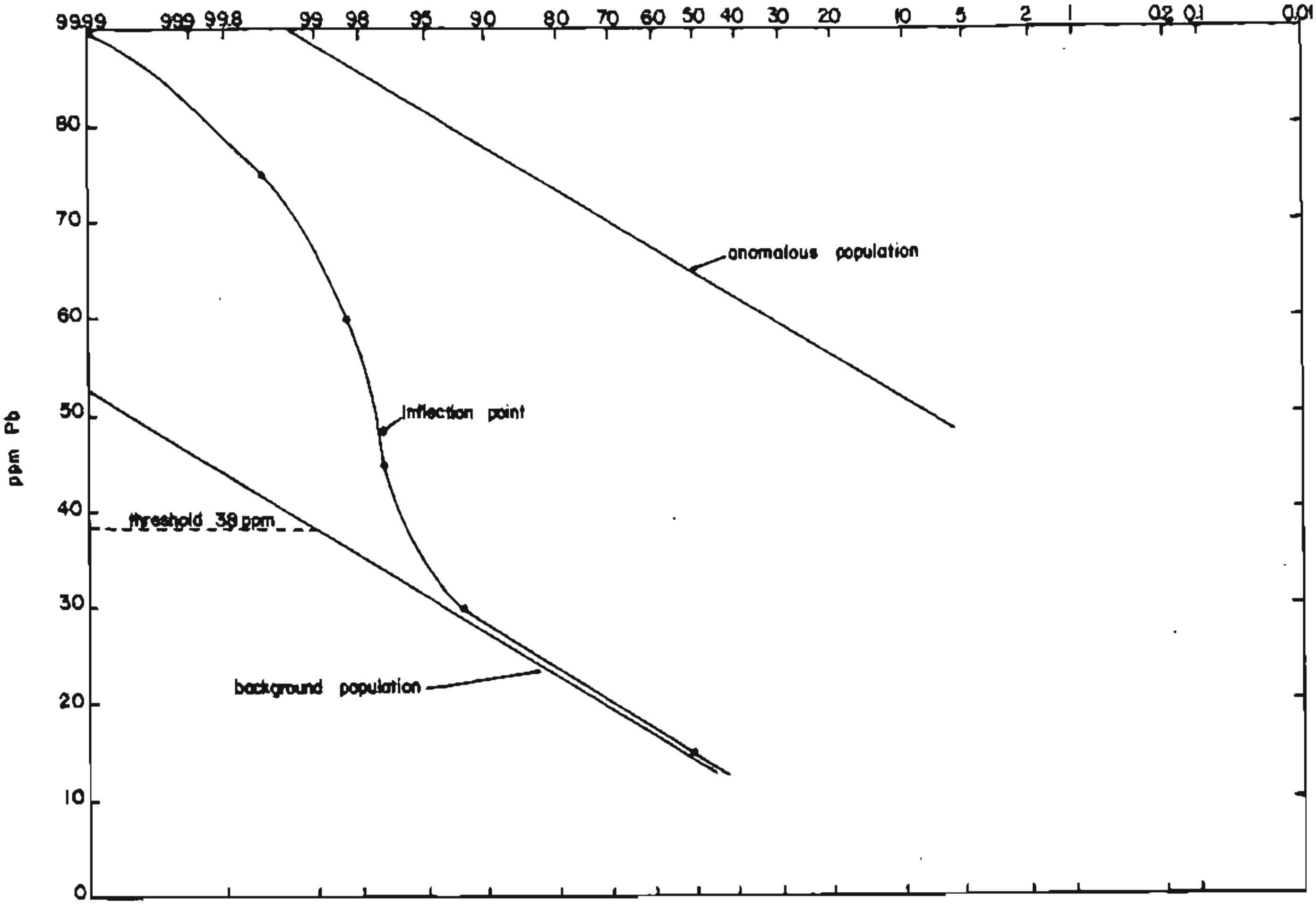

Figure 16. Cumulative probability plot of lead distribution, Silver Fox Mine, Fairbanks mining district, Alaska.

The anomaly at 12E-9N is barely above threshold, with the maximum value reaching 36 ppm. No other elements reach anomalous proportions in this area. However, the sample does occur adjacent to a partially mineralized pit and may be a false anomaly. On line 2E sample 16N, a value of 31 ppm was obtained. This sample occurs away from all known excavations and is probably a true anomaly. The sample site occurs within the Birch Creek schist. No mineralization other than stibnite and gold has been recognized in these rocks on the Silver Fox Mine property. On line 10E-14N, a sample with 33 ppm copper was collected. This is not much above threshold, but no apparent source of contamination exists, and the anomaly should be investigated further.

No obvious trends are apparent in the copper distribution except that most values above 25 ppm occur over the quartz diorite. No such values are present over the Fox Creek pluton. This was anticipated because no sulfide mineralization of note has been exposed in the quartz monzonite.

Figure 20 shows the relationship of the lead distribution to the geology. Five anomalies occur over the survey area, and all but one occur in the quartz diorite. Sample 5E-7N contains 70 ppm lead and is surrounded by lower anomalous values. This sample occurs within the contact hornfels zone of the Fox Creek pluton. The area is characterized by quartz-biotite schist cut by

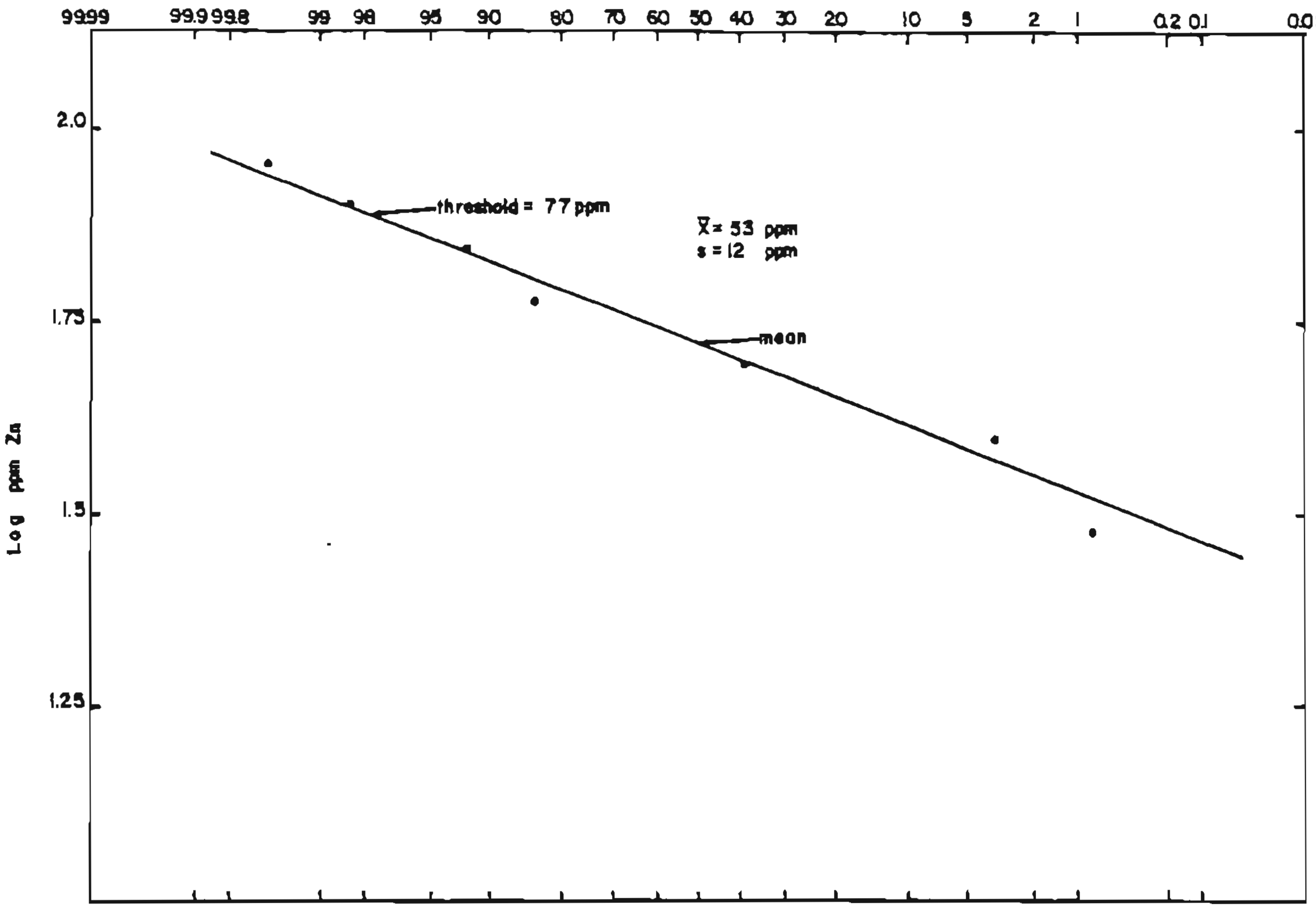

Figure 17. Log-cumulative probability plot of zinc distribution, Silver Fox Mine, Fairbanks mining district, Alaska.

quartz monzonite dikes that range from 2 to 10 cm in width. Molybdenum and silver are also anomalous at this site (figs. 21, 22). Anomalies centered at 13E-13N and 15E-7N are apparently the result of dispersion from mineralized pits and the mine dump. Trenching at 13E-13N revealed no mineralization or alteration of the quartz diorite. The moderate anomalies, at 16E-13N and 16E-14N may be true anomalies, although these sample sites are directly downslope from the mineralized area of location 1 (pl. 1). Trenching may be warranted to confirm the above.

The anomaly at 15E-16N should be investigated because it is away from mineralized areas and is probably not the result of contamination. Sample 13E-9N (68 ppm) occurs near the road and may be contaminated because mineralized material is scattered about the general vicinity. Trenching of the above sites could easily verify the presence of mineralization.

Lead is similar to copper in that it tends to be more concentrated within the quartz diorite. The anomalies of prime interest are those at 5E-7N and 15E-16N because they are least likely to be the result of contamination. The soil survey was successful in outlining the dispersion trains of known mineralized areas, although the periphery of some of these anomalies may warrant closer inspection.

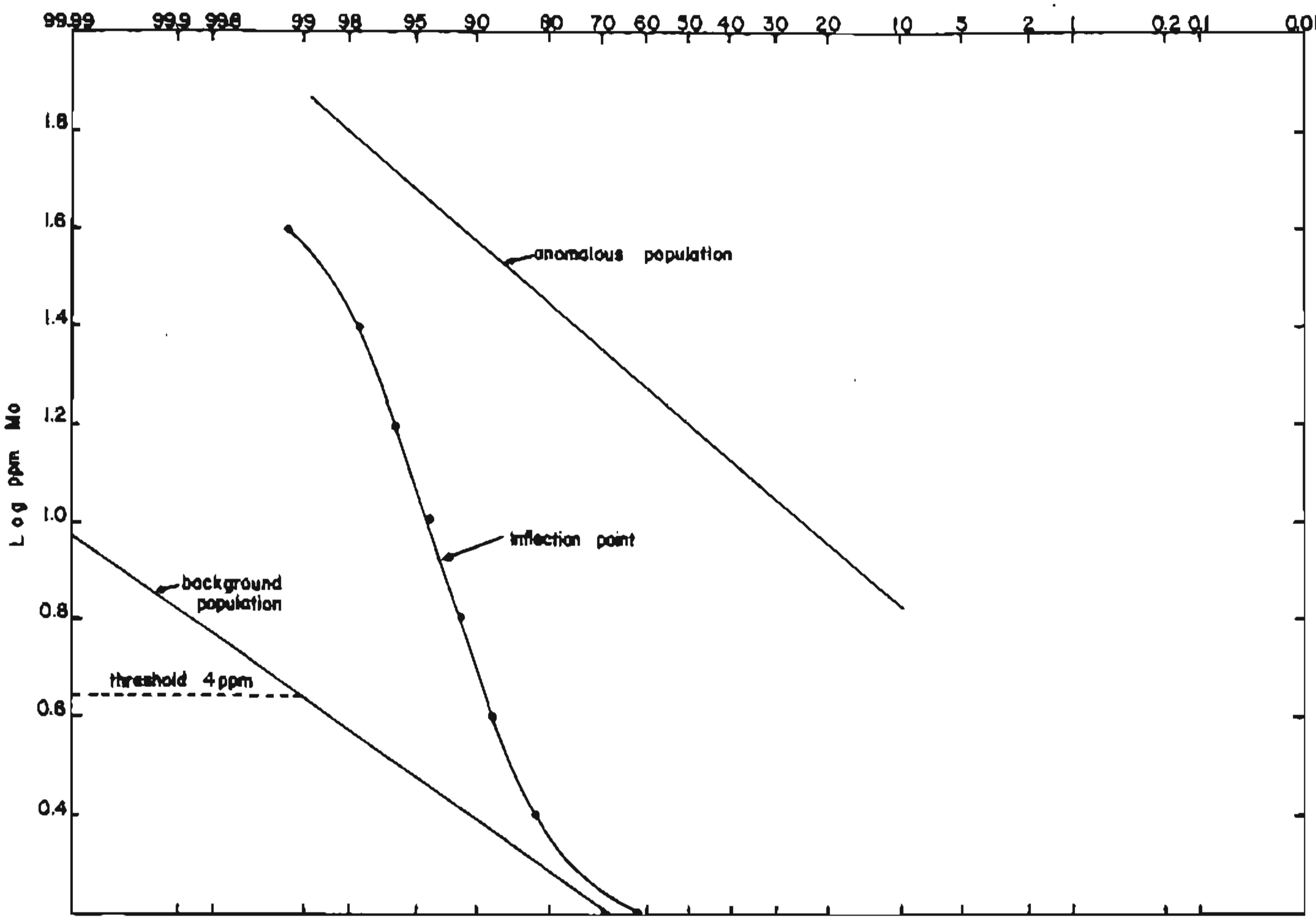

Figure 18. Log-cumulative probability plot of molybenum distribution, Silver Fox Mine, Fairbanks mining district, Alaska.

Figure 23 shows the zinc distribution over the survey grid. Of the four areas anomalous in zinc, two were rejected as false because they occur at the same locations as false lead anomalies. Anomalies centered at 14E-6N and 14E-14N are associated with known mineralization and coincide closely with the lead anomalies in the same area (fig. 20).

The anomalous area centered at 11E-6N contains a high of 86 ppm zinc, but is adjacent to a mineralized pit and is probably the result of dispersion. Sample 7E-6N contains 90 ppm zinc and is associated with an excavation area subject to runoff and erosion. Although no specific zinc mineralization occurs within the pit---in quartz monzonite---the validity of the anomaly should be considered suspect. A small lead anomaly of 40 ppm occurs primarily within the pit area upslope from the zinc anomaly on line 7E.

Zinc tends to be anomalous within the quartz diorite. The anomaly within the quartz monzonite is undoubtedly due to dispersion from the pit. Correlation of zinc and lead anomalies is fairly good; three of the four zinc anomalies are associated with lead.

Figure 21 shows the molybdenum distribution over the survey grid. Two anomalous areas are present, the largest spanning lines 3E through 8E and 1N through 8N. Sample 4E-2N and 5E-6N contain 42 ppm and 44 ppm molybdenum, respectively. The area encompassed by the large anomaly is typically under-

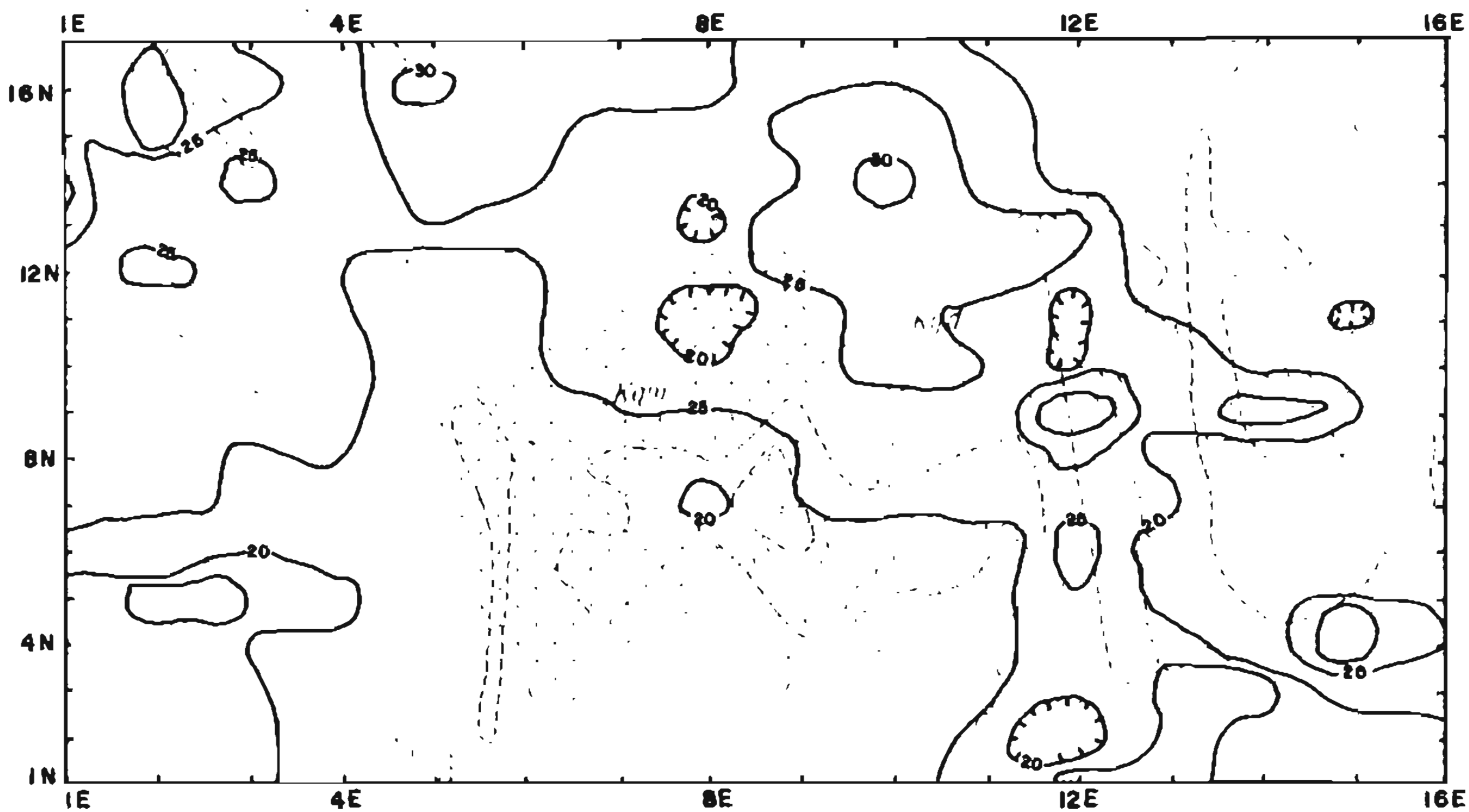

Figure 19. Contour map of the copper distribution over the survey grid shown on plate 1, Silver Fox Mine, Fairbanks mining district, Alaska.

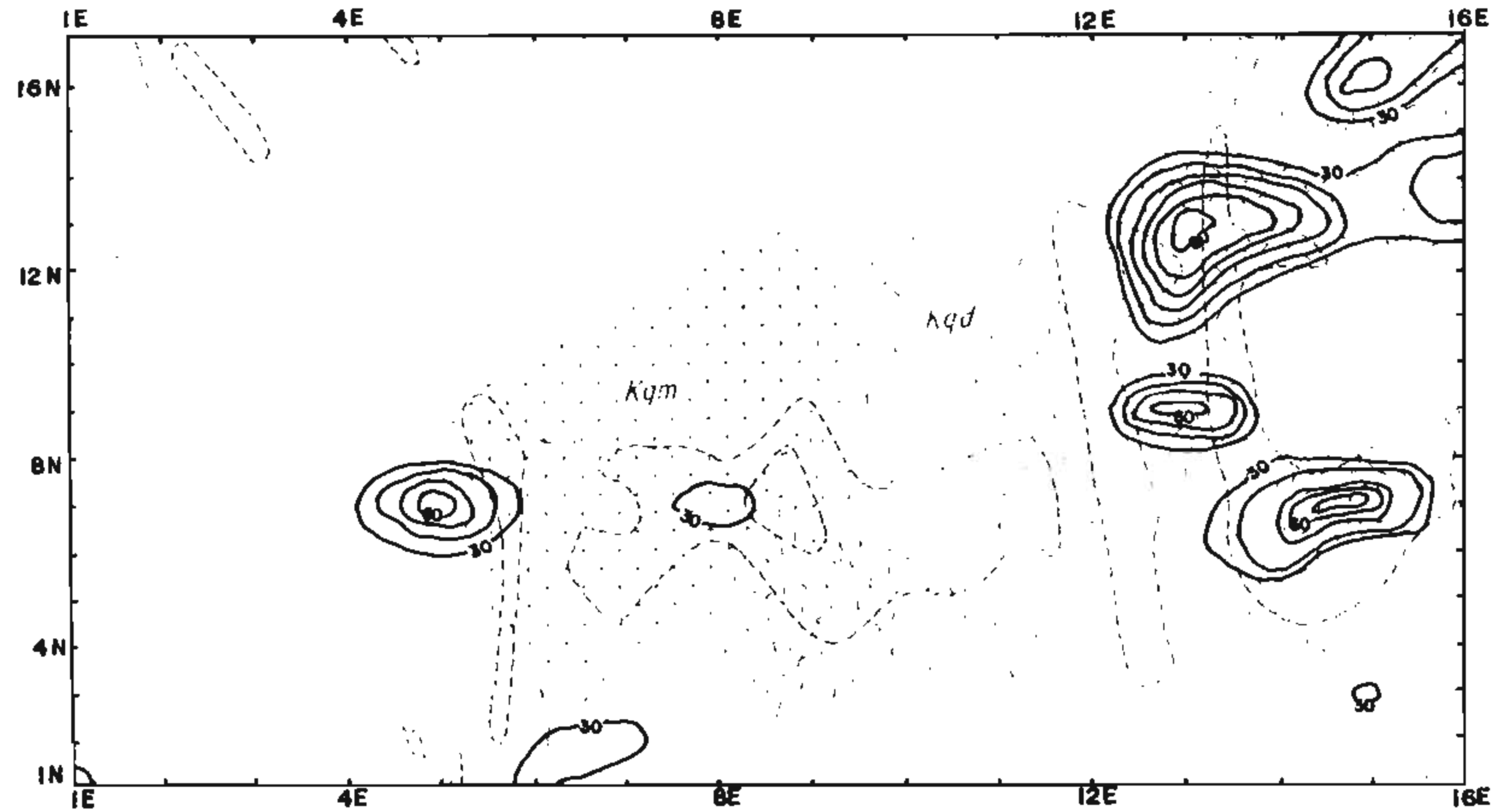

Figure 20. Contour map of the lead distribution over the survey grid shown on plate 1, Silver Fox Mine, Fairbanks mining district, Alaska.

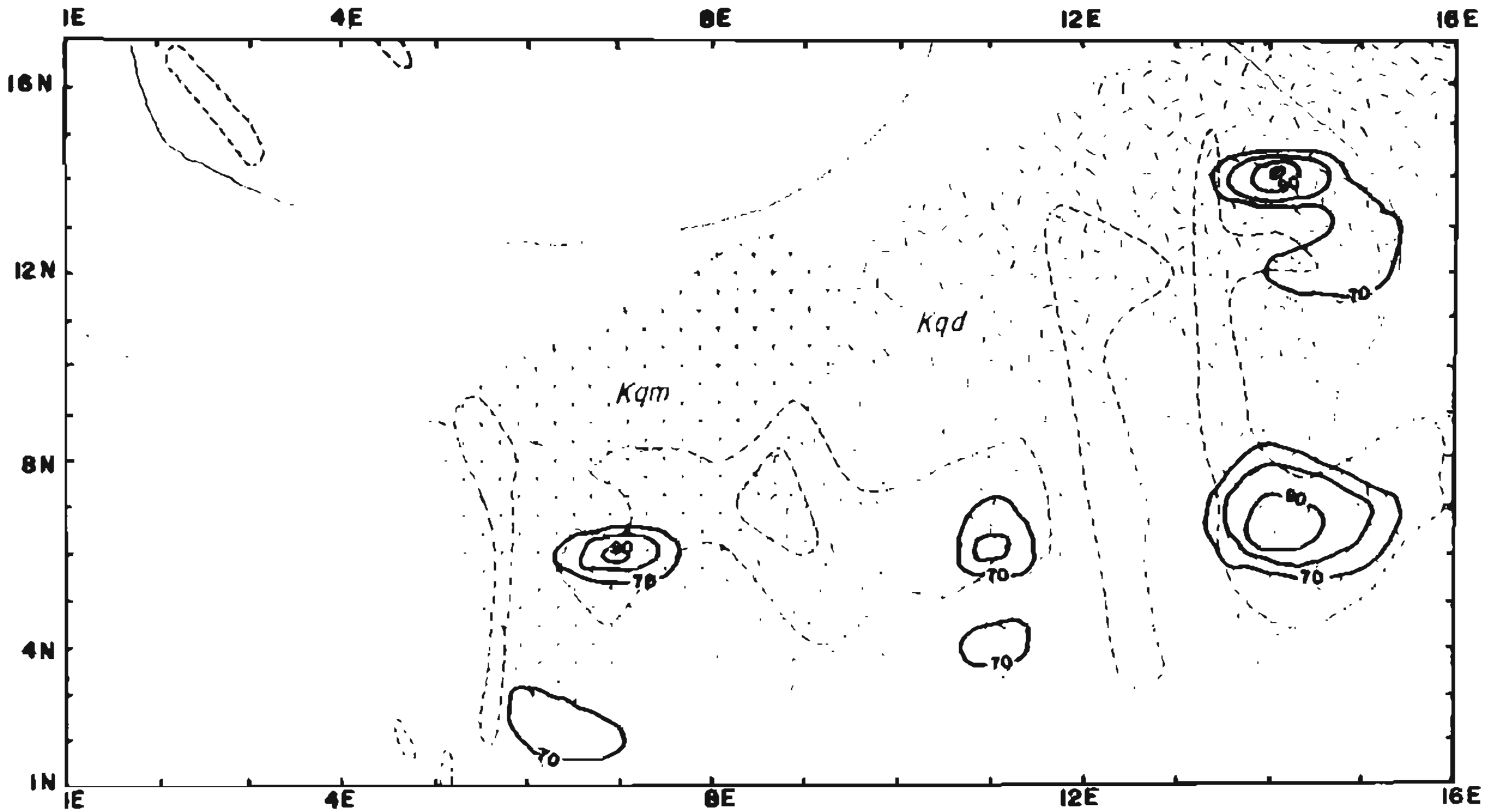

Figure 21. Contour map of the molybdenum distribution over the survey grid shown on plate 1, Silver Fox Mine, Fairbanks mining district, Alaska.

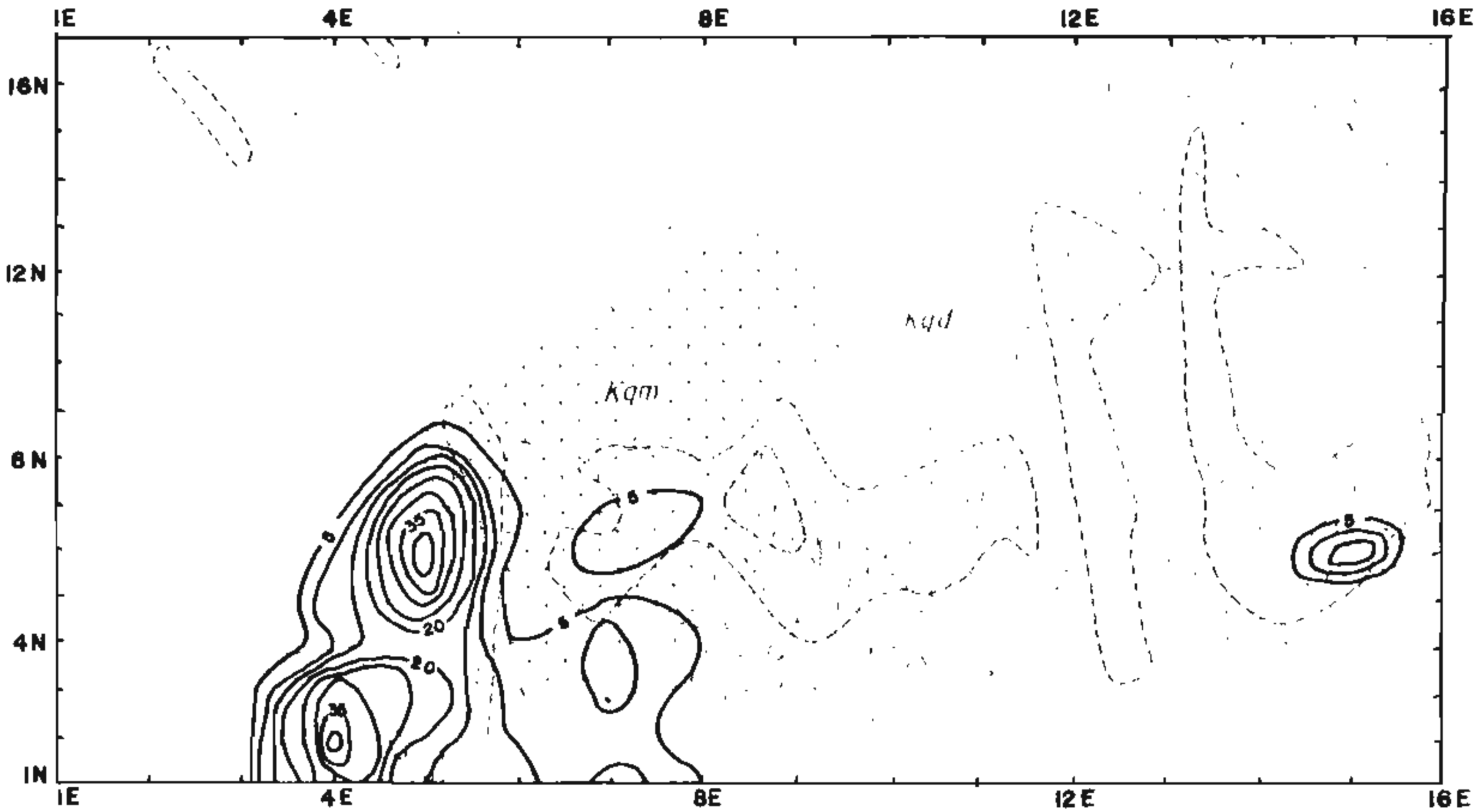

Figure 22. Contour map of the silver distribution over the survey grid shown on plate 1, Silver Fox Mine, Fairbanks mining district, Alaska.

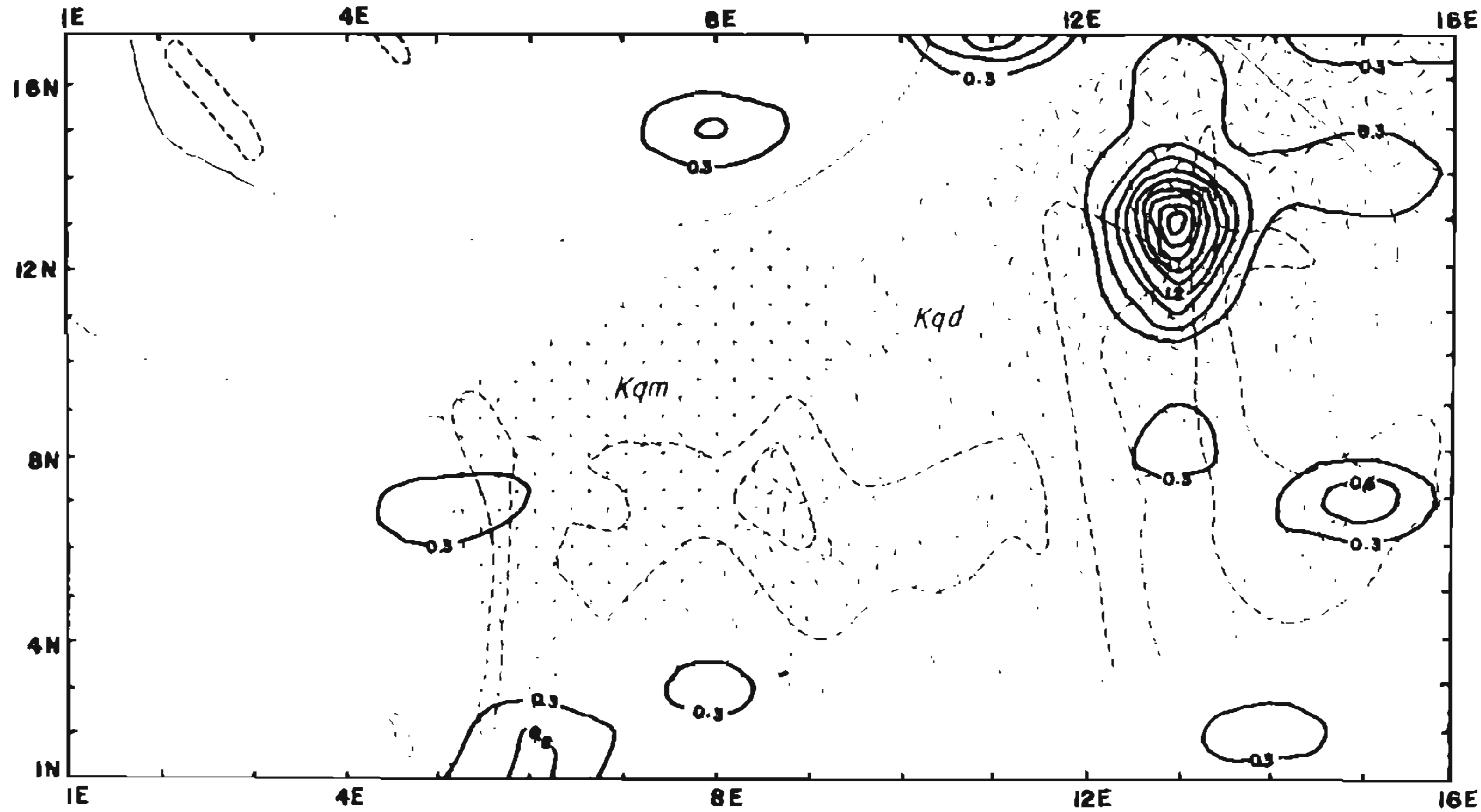

Figure 23. Contour map of the zinc distribution over the survey grid shown on plate 1, Silver Fox Mine, Fairbanks mining district, Alaska.

lain by the contact quartz-biotite hornfels that is cut by quartz monzonite dikes. A hand-dug hole in the region of 5E-6N revealed no mineralization, but rocks that match the above description were present. This anomalous area may be relatively enriched in molybdenum within the contact zone of the quartz monzonite.

The other anomaly of note occurs at 15E-6N and contains 18 ppm molybdenum. This sample is similar to others in that it occurs adjacent to a mineralized area and hence may be the result of dispersion.

The concentration of molybdenum along lines 3E through 8E is interesting. A random grab sample of quartz monzonite (102-3, pl. 1) showed 'background' values of 14 ppm copper, 2 ppm molybdenum, and 15 ppm tungsten. Sample 102-3 is located approximately 350 ft from the 44 ppm molybdenum high and indicates that significant molybdenum enrichment must be present below the anomalous area. Sample 103-3 is from a quartz vein in schist that occurs within the contact zone. This sample contains 32 ppm copper, 134 ppm molybdenum, 360 ppb gold, and 115 ppm antimony. This sample lies within the anomalous zone and further illustrates the enrichment in the bedrock.

Figure 22 is a contour map of the silver distribution. Several anomalies can be classified as false because other elements showed false anomalies in the same areas. The large anomalies centered at 13E-13N and 15E-14N coincide with lead anomalies that are probably caused by contamination from mineralized pits. The smaller anomaly at 15E-7N also falls in the above category.

The anomaly at 5E-7N corresponds to a lead and molybdenum anomaly; though only 0.4 ppm is present it is still significant. The anomalies at 8E-15N and 11E-17N are not associated with known mineralization and they do not correspond with any lead, zinc, or copper anomaly. These should be investigated to determine if they are significant.

Silver anomalies show a random distribution with regard to rock type. Of the anomalies considered valid, two apparently occur within the Birch Creek schist and one occurs within the quartz monzonite. At present, the only known argentiferous veins occur in the quartz diorite.

General Comments on Anomalies

The anomalies defined by the survey are generally associated with known mineralization. Of those that are not, the large molybdenum and associated lead, silver, and zinc anomalies are of greatest interest.

The elevated values of all elements at 6E-1N, 6E-2N, and 7E-1N may be the result of a break-in-slope anomaly. At this point, the hill abruptly flattens into the Fox Creek drainage. This area should be re-examined to determine the precise cause of the anomaly.

Attempts were made to eliminate false anomalies on the basis of their relation to mineralized excavations. Time did not allow the confirmation of the above anomalies, but in many cases it is possible that an anomaly adjacent to a known vein or mineralized area may indeed represent other unexposed bedrock mineralization.

Magnetic Survey

A magnetic survey was conducted in conjunction with the geochemical sampling program to determine if any unique geomagnetic signature was present over the sample area. Readings were taken on the N 25° E lines at 50-ft intervals using a proton precession magnetometer (app. D).

The total magnetic field data was converted to vertical magnetic field (Z) data using an inclination of 77 degrees as determined from the College Observatory. Drift variations were corrected using the records from the College Observatory, located approximately 15 mi from the mine site.

Figure 24 is a computer-generated magnetic contour map. The most striking trend is the concentration of values that are less than the 55,500-gamma base contour in the southeastern portion of the sample area. Although the entire mineralized area is not characterized by these relatively lower values, areas 'A' and 'B' are regions of relative magnetic lows and both occur in mineralized pits. Sulfide minerals tend to have a low magnetic susceptibility and can sometimes be located by means of a detailed survey (Telford and others, 1976). The altered rocks of the mineralized pits may also have caused lower readings because of the destruction of higher susceptibility mafic minerals. Thus, these two relative magnetic lows may result from combined characteristics of the sulfide minerals and the altered wallrock. The 200-ft spacing causes an uneven data interval in the roughly east-west direction. Hence, the width of the low regions was probably exaggerated during contouring. Examination of the data for line 10E (area 'A') shows a low of 55,380 gammas at point 12N. Values north and south of this are also low but increase away from the 55,380 minimum. These two anomalous lows are therefore the result of alteration and possible sulfide-mineral accumulations.

The anomalous high in the northwestern region of the sample area is unexplained because it apparently occurs within the Birch Creek schist. No data were collected for line 2E; hence, the contouring process may have exaggerated the width of the anomaly.

In terms of a porphyry model, a magnetic high in the peripheral regions of the phyllic zone might be expected. The relative high that occurs adjacent to the low on line 10E falls in the loosely defined potassic alteration zone, although it is quite close to the sericitic zone.

In general, it does not appear that the magnetic features can be related to a classical porphyry system. The lows appear to represent altered mineralized areas in which the ferromagnesian minerals have been generally depleted.

SUGGESTIONS AND RECOMMENDATIONS

The following speculations on the mineral potential of the Silver Fox Mine area are made in the context of current knowledge of the area from this and previous studies.

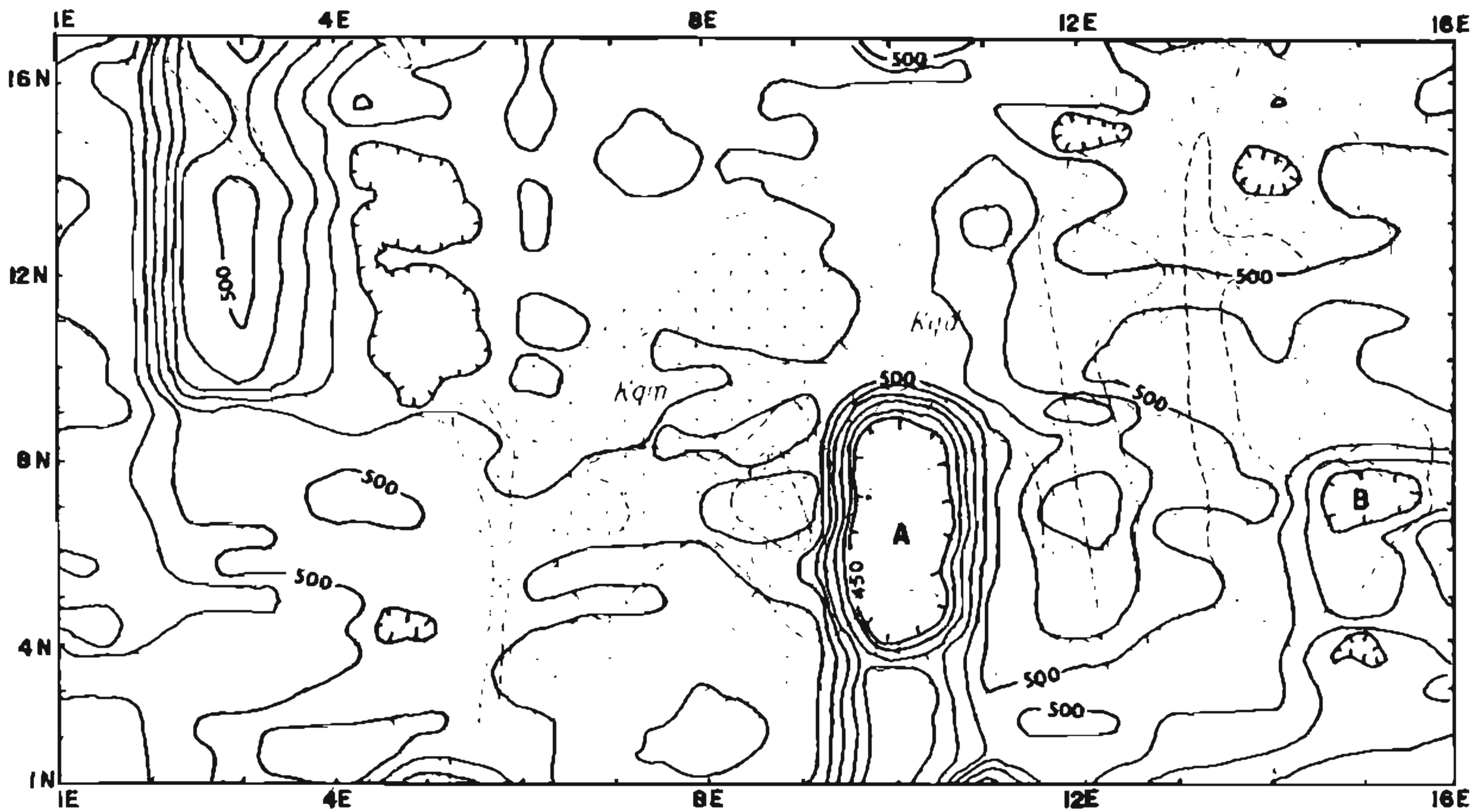

Figure 24. Contour map of the geomagnetic values over the survey grid shown on plate 1 (base contour is 55,000 gammas); Silver Fox Mine, Fairbanks mining district, Alaska.

Sulfide-vein Potential

Sulfide veins are exposed at locations 3, 4, and 5 on the surface (pl. 1) and in the underground workings (pl. 2). Of these locations, 3 and 4 have been mined out by surface methods to the near-practical limit. The underground vein has been exposed by drifting during development work (as shown on pl. 2) and no stoping has been done. Location 5 contains sulfides in an irregular reticulating-vein system, and further excavation is required to determine if they could be successfully mined at a small scale. Presently the underground vein appears to be the only one readily amenable to mining.

Several factors affect the mineability of the sulfide veins. The narrow vein width requires relatively high-grade ore for a profitable mining venture. Two chip samples across a hypothetical mining width of 3 ft were taken underground to evaluate the expected mineable grade. Table 1 lists the results of these samples. In a mining operation of this nature, precious metals would be of primary interest because tonnages will probably be low and lead-zinc production on an economic scale is not possible. Gold values range from 0.1 to 1.9 ppm and silver ranges from 2.3 to 6.6 ounces per ton, making the value per ton of ore less than $100 at present prices. This value per ton is probably not high enough to maintain the small-scale mining operation that would be required given the apparently low tonnages.

Because the veins are often joint fillings, they tend to be discontinuous and subject to local pinching and swelling. Faulting is a major consideration in the feasibility of an operation where grade and tonnage are critical factors. Figure 10 shows a map of location 3 (pl. 1) where three subparallel veins existed prior to opencast mining. These veins were isolated both laterally and vertically by faulting, and cut off to the west by a shear zone and to the east by a steeply dipping fault. The extension of these veins has not been located on either side of the faults. If this situation can be considered typical, mine planning and development would be difficult, especially in view of the vein width and grades involved.

Sulfide veins presently exposed appear marginal as a target for underground development. It is not likely that underground development would be profitable. High-grading of surface exposures may be profitable in a very limited sense because pit development below a depth of 18 to 20 ft becomes uneconomical in terms of mining a 4 to 12 in. vein. Further exploration may reveal veins that could warrant underground development, but structural constraints will probably adversely affect any mining effort unless widths and grades are considerably greater than those currently exposed.

Low-grade Gold Potential

Forbes and others (1968) sampled the reticulated-vein system in the quartz diorite (fig. 25) and suggested that this area may be amenable to bulk mining for gold. Six channel samples were taken over the mineralized area to obtain a representative analysis of the vein system. Table 4 lists these results and those from three grab samples of the vein material.

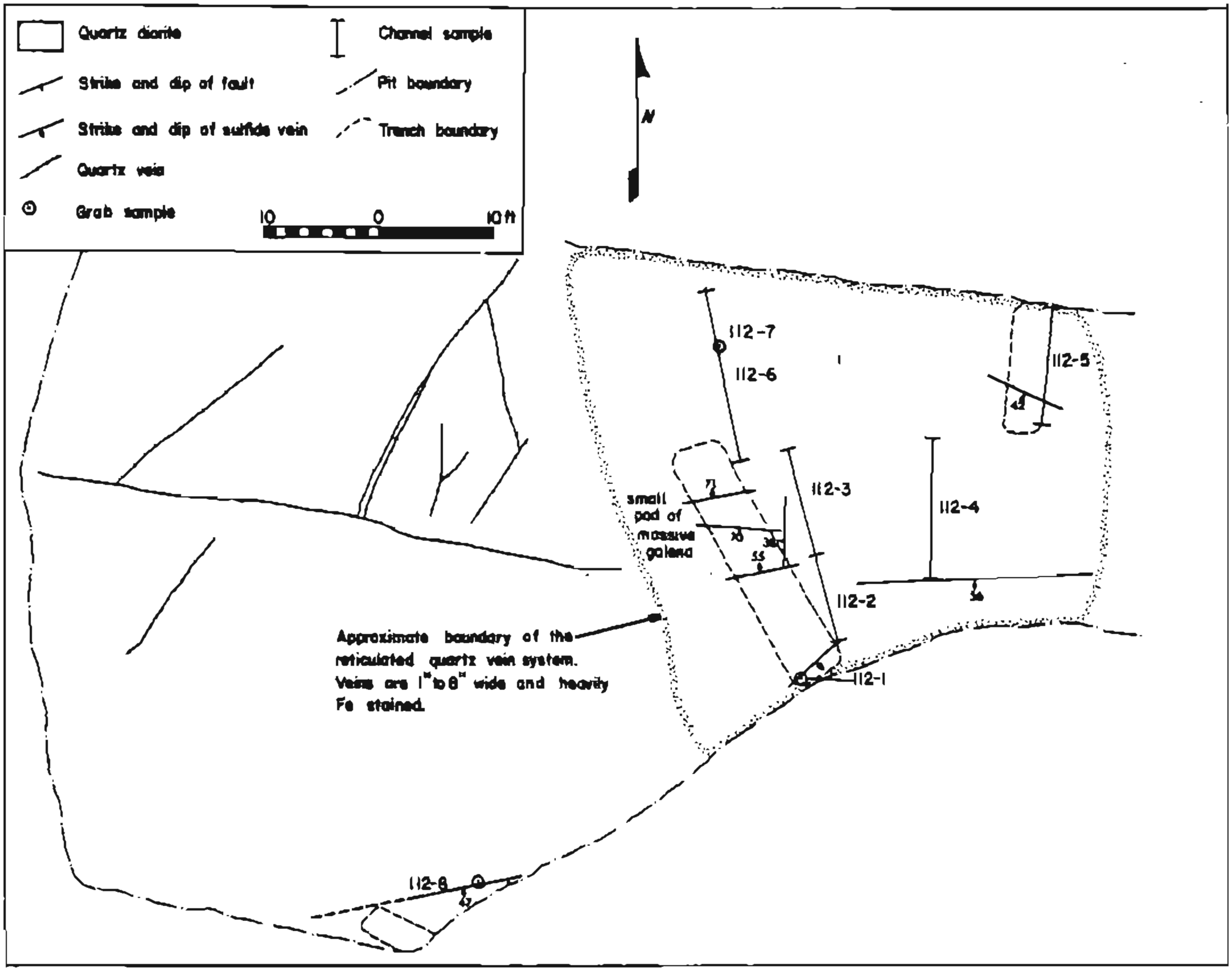

Figure 25. Pit map of the reticulated-vein system in the quartz diorite (loc. 5, pl. 1), Silver Fox Mine, Fairbanks mining district, Alaska.

Table 4. Atomic-absorption analyses of samples from the reticulated-vein system in quartz diorite. All values in ppm unless otherwise noted.

Sample no.	Sample type	Cu	Pb	Zn	Mo	Au	Ag	Sb
112-1	grab	362	5.6%	2400	228	4.5	500	1050
112-2	channel (8 ft)	103	2.35%	3100	121	0.8	79	246
112-3	channel (10 ft)	54	3110	3800	24	0.3	24	70
112-4	channel (13 ft)	63	3110	5200	20	0.1	21	47
112-5	channel (10.5 ft)	112	2185%	1400	99	0.8	91	224
112-6	channel (15.5 ft)	69	9410	3800	132	0.5	32	95
112-7	grab	155	6.30%	1200	520	7.5	226	560
112-8	grab	78	3890	4100	77	0.7	38	118

Weighting the samples on a foot-assay product basis yields an average of 0.014 ounce per ton gold, 1.34 ounce per ton silver, 0.012 percent copper, 1.259 percent lead, 0.358 percent zinc, 0.008 percent molybdenum, and 0.025 percent antimony. Using values of $500 per ounce for gold and $10 per ounce for silver, the material has a precious-metal value of approximately $20 per ton, a value not high enough to sustain mining. Grab samples of sulfide veins were not included in these averages and although they will add to the overall grade of the material, the effect is probably not enough to bring the grade up to an economic level. Potential for high-grading the veins is present, although bulk mining of the entire reticulated system does not appear feasible.

Potential for Molybdenum and Copper Production

Any estimates of the potential for molybdenum and copper production are based on limited observations, specifically in that portion of the mineralized stockwork exposed underground and the one occurrence of chalcopyrite and molybdenite at location 38-2 (pl. 1).

As stated previously, molybdenite occurs as both disseminations and smeared surface coatings on the quartz-stockwork contacts. While in many cases the amount of molybdenite is appreciable, the grade of the stockwork and host is too low to be economic. Typical molybdenum stockworks average 1500 to 5000 ppm molybdenum; samples from the Silver Fox Mine ran 8 to 11 ppm, with copper from 9 to 14 ppm (table 2). These values are far lower than those required for ore-grade material.

Only a small portion of the stockwork is exposed; hence, an evaluation on the basis of only limited information is tenuous. Diamond drilling could be used to test the molybdenum mineralization at depth if there is sufficient interest in the stockwork. An induced-polarization survey over the quartz diorite near and around the mine may provide a more competent data base on which to draw conclusions. The alteration assemblages at the mine are similar to those found in other molybdenum stockworks; hence, there may be a possibility for stronger mineralization at depth.

The presence of chalcopyrite and molybdenite in sample 38-2 seems to indicate that the mineralization may have some areal extent, although no direct correlation between the underground stockwork and this occurrence can be made because of inadequate exposure.

While the alteration observed on the property does not fit the classic copper-porphyry model of Lowell and Gilbert (1970), few molybdenum or copper porphyries do. This fact does not preclude the possibility of economic mineralization, but based on this study, it appears that the molybdenum occurrence may be locally concentrated in suitable structures because little molybdenum has been found on the surface. Mineralization at depth depends on the stockwork character and the intensity of the mineralizing event, two factors that cannot be assessed without drilling or further underground development.

COMPARISON WITH OTHER MOLYBDENUM STOCKWORKS

Stockwork-molybdenum deposits have been classified into calc-alkalic, high-potassium calc-alkalic (Climax type), and alkalic (Westra and Keith, 1981). Calc-alkaline deposits tend to be small, low-grade deposits exhibiting low fluorine and tin levels. Alkalic deposits include the Climax type and are generally higher grade, larger tonnage deposits located in a back-arc spreading environment. Typical host rocks for the alkalic-type deposits include rhyolite, quartz latite, granite, monzonite, syenite, and leucogranite.

The calc-alkaline-type deposits have been divided on the basis of host into stock and plutonic types. These deposits have also been termed granodiorite-molybdenum systems by Mutschler and others (1981). In terms of alteration and mineralization, these systems show a closer relationship to Cordilleran porphyry-copper deposits than to alkalic molybdenum stockworks.

The Silver Fox Mine system can be classified as a calc-alkalic molybdenum stockwork. Table 5 compares some of the aspects of a typical calc-alkalic stockwork to that of the Silver Fox Mine.

Table 5. Comparison of a typical calc-alkalic stockwork molybdenum deposit with the Silver Fox Mine, Fairbanks mining district, Alaska.

Aspect	Typical deposit	Silver Fox Mine
Host rock	Quartz diorite granodiorite	Quartz diorite to quartz monzonite
Alteration	Potassic, phyllic, argillic, propylitic	Potassic, weak phyllic, poorly defined argillic, propylitic
Tectonic setting	Convergent plate margin	Continental crust
Porphyry textures	Yes	Yes
Flourine	Low	Low to absent, no macroscopic evidence
Tin	Trace	Absent(?)
Tungsten	Scheelite	Scheelite
Molybdenum grade	0.1 to 0.25%	<0.1%
Associated minerals	Pyrite with minor chalcopyrite, galena, sphalerite, and pyrrhotite	Pyrite, major sulfide veins of galena, sphalerite, and pyrite

CONCLUSIONS

The mineralization at the Silver Fox Mine is the result of two mineralizing events, the first associated with the quartz diorite intrusive, and the second with the quartz monzonite. The mineralization in the quartz diorite appears to represent a collapsing hydrothermal system as evidenced by the presence of high and low temperature phases in close proximity. Cooling of the quartz diorite resulted in deposition of molybdenite through fissure-vein sulfides as the stability fields changed as a function of temperature. The differentiation of the quartz monzonite resulted in the potassium-feldspar alteration phase that affected both the quartz diorite and the quartz monzonite.

Alteration assemblages are similar to those in porphyry systems although they tend to be weakly developed. The stockwork mineralization and alteration is considered the result of a weakly developed porphyry system that thermally collapsed on itself. Because the portion of the intrusive exposed appears to be the hood zone, the character of the alteration and mineralization at depth may be quite different. Thus, additional underground information is necessary to definitively evaluate the occurrence. Diamond drilling would resolve the nature of the stockwork character at depth.

At the present time, the potential of the mine is limited to high-grading of surface exposures of the sulfide veins and possibly the development of the vein underground. The principle deterrents to mining are the narrow, discontinuous nature of the veins and the relatively low tonnages.

REFERENCES CITED

Anonymous, 1913, Tanana Magazine, quartz edition.

Britton, J.M., 1969, Petrology and petrography of the Pedro Dome plutons, Alaska: Fairbanks, University of Alaska M.S. thesis, 41 p.

Brown, J.M., 1962, Bedrock geology and ore deposits of the Pedro Dome area, Fairbanks mining district, Alaska: Fairbanks, University of Alaska M.S. thesis, 137 p.

Chapman, R.M., Weber, F.R., and Taber, B., 1971, Preliminary geologic map of the Livengood Quadrangle, Alaska: U.S. Geological Survey Open-file Report 71-66, 2 sheets.

Clark, K.F., 1972, Stockwork molybdenum deposits in the western Cordillera of North America: Economic Geology, v. 67, p. 731-758.

Forbes, R.B., 1982, Bedrock geology and petrology of the Fairbanks mining district, Alaska: Alaska Division of Geological and Geophysical Surveys Open-file Report 169, 68 p.

Forbes, R.B., and Brown, J.M., 1961, A preliminary map of bedrock geology of the Fairbanks mining district, Alaska: Alaska Division of Mines and Minerals Report 194-1.

Forbes, R.B., Pilkington, H.D., and Hawkins, D.B., 1968, Gold gradients and anomalies in the Pedro Dome-Cleary Summit area: U.S. Geological Survey Open-file Report, 43 p.

Forbes, R.B., and Weber, F.R., 1982, Bedrock geologic map of the Fairbanks mining district, Alaska: Alaska Division of Geological and Geophysical Surveys Open-file Report 170, 2 pl.

Foster, H.L., Weber, F.R., Forbes, R.B., and Brabb, E.E., 1973, Regional geology of the Yukon-Tanana Upland, Alaska, in Arctic Geology: American Association of Petroleum Geologists Memoir 19, p. 388-395.

Hawkes, H.E., and Webb, J.S., 1962, Geochemistry in Mineral Exploration: Harper and Row, New York.

Hill, J.M., 1933, Lode deposits of the Fairbanks district, Alaska: U.S. Geological Survey Bulletin 849-B, p. 29-163.

Lowell, J.D., and Gilbert, J.M., 1970, Lateral and vertical alteration-mineralization zoning in porphyry ore deposits: Economic Geology, v. 65, p. 373-408.

Meyer, C., and Hemley, J.J., 1967, Wall-rock alteration, in Barnes, H.L., ed., Geochemistry of hydrothermal ore deposits: New York, Holt, Rinehart, and Winston, p. 166-235.

Mowatt, T.C., 1974, Petrologic studies in the Fairbanks district: Molybdenum mineralization at the Silver Fox Mine: Alaska Department of Geological and Geophysical Surveys Open-file Report 46, 29 p.

Mutschler, F.E., Wright, E.G., Ludington, S., and Abbot, J.T., 1981, Granite molybdenum systems: Economic Geology, v. 76, p. 874-897.

Prindle, L.M., Katz, F.J., and Smith, P.S., 1913, A geologic reconnaissance of the Fairbanks Quadrangle, Alaska: U.S. Geological Survey Bulletin 525, 200 p.

Sinclair, A.J., 1976, Applications of probability graphs in mineral exploration: B.C., Canada, Association of Exploration Geochemists, v. 4, 95 p.

Swainbank, R., 1971, Geochemistry and petrology of eclogitic rocks in the Fairbanks area, Alaska: Fairbanks, University of Alaska Ph.D thesis.

Telford, W.M., Geldart, L.P., Sheriff, R.E., and Keys, D.A., 1976, Applied geophysics: New York, Cambridge University Press, 860 p.

Westra, G., and Keith, S.B., 1981, Classification and genesis of stockwork molybdenum deposits: Economic Geology, v. 76, p. 844-873.

APPENDIX A

Q-A-P diagram and modes for typical intrusive rocks in the Silver Fox Mine area, Fairbanks mining district, Alaska.

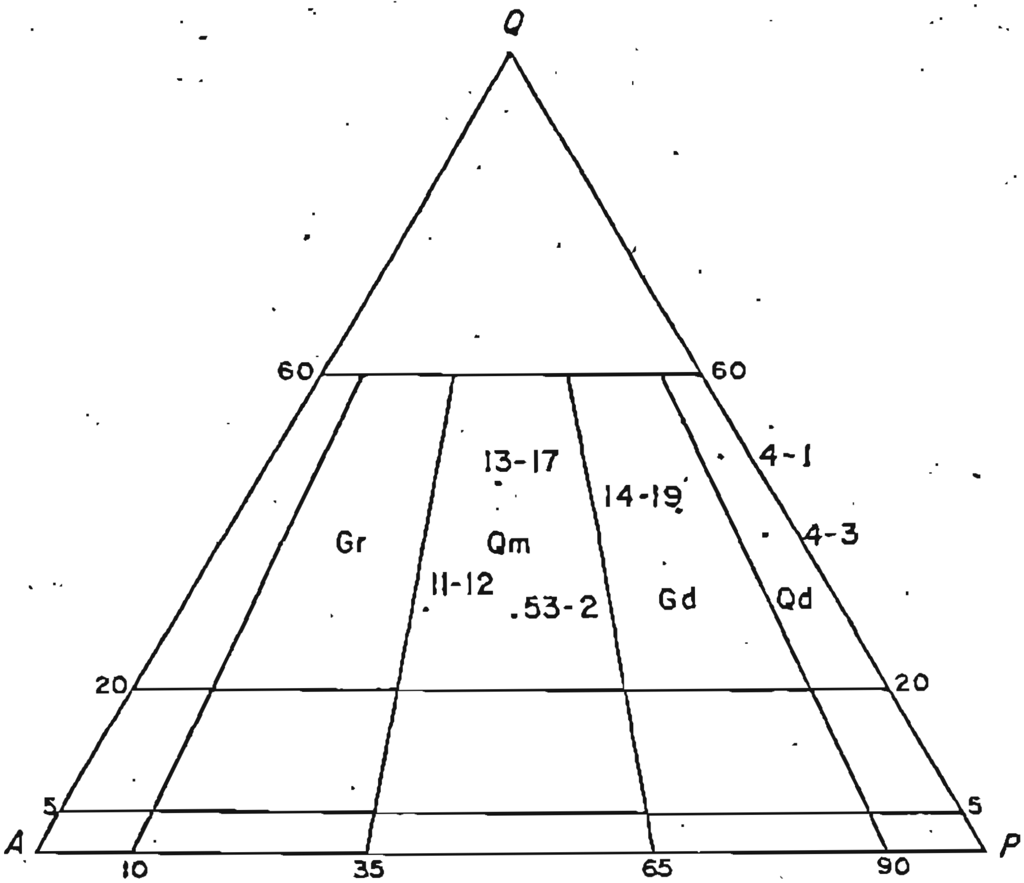

Sample #	Quartz	K-feldspar	Plagioclase
4-1	49%	3.8%	47.2%
4-3	37%	4.0%	59.0%
11-12	31%	42.5%	26.5%
13-17	45%	27.0%	28.0%
14-19	42.2%	11.8%	46.0%
52-3	32.7%	30.5%	36.8%

Gr -- Granite
Qm -- Quartz monzonite
Gd -- Granodiorite
Qd -- Quartz diorite

APPENDIX B

Summary of rock and mineral analyses.

Sample #	Cu	Pb	Zn	Mo	Au	Ag	W	Sb
36-1	680	9900	1160	8	70	975	-	-
36-2	36	8900	2100	4	11.7	663	-	-
36-3	130	8100	3500	20	13.3	345	-	-
36-3.1	310	6800	1030	26	-0.1	85	-	-
36-3.2	390	8900	1190	9	10.9	660	-	-
36-3.3	230	9700	2500	18	1.3	135	-	-
36-4	43	6700	340	51	1.6	41	-	-
36-4.1	690	10100	1800	260	7.2	165	-	-
38-1	130	9700	240	16	2.4	195	-	-
38-2	1900	1040	330	130	-0.1	9	-	-
39-1	460	7900	152	170	0.5	49	-	-
39-1.1	33	620	210	45	0.3	4	-	-
60-1	100	7700	19400	5	-0.1	79	-	-
60-2	260	6500	39000	3	1.9	228	-	-
60-3	14	146	81	11	-0.1	2	-	-
60-4	13	490	93	9	-0.1	1	-	-
70-2	4000	9000	800	19	2.9	1120	-	-
102-3	14	-	-	2	-	-	15	-
103-3	32	-	-	134	0.36	-	-	115
105-2	4	60	9	4	-0.1	0.2	-	-
105-3	21	68	39	43	-0.1	0.2	-	-
107-1	149	29600	1600	35	0.83	91.9	-	-
107-3	9	-	-	8	-	-	35	-
107-4	760	95500	37600	6	1.4	662	-	-
112-1	362	5.6%	2400	228	4.5	500	-	1050
112-2	103	2.35%	3100	121	0.8	79	-	246
112-3	54	3110	3800	24	0.3	24	-	70
112-4	63	3110	5200	20	0.1	21	-	47
112-5	112	2.95%	1400	99	0.8	91	-	224
112-6	69	9410	3800	132	0.5	32	-	95
112-7	155	6.3%	1200	520	7.5	226	-	560
112-8	78	3890	4100	77	0.7	38	-	118

"-" indicates no analysis requested.

All values in ppm.

APPENDIX C

Geochemical soil-sample analyses (all values in ppm).

EAST	NORTH	Cu	Pb	Zn	Mo	Ag
1	1	20.00	35.00	62.00	1.00	0.20
1	2	21.00	20.00	54.00	1.00	0.20
1	3	27.00	20.00	69.00	0.	0.20
1	4	22.00	15.00	57.00	1.00	0.20
1	5	22.00	12.00	55.00	1.00	0.20
1	6	18.00	13.00	51.00	1.00	0.20
1	7	23.00	13.00	59.00	2.00	0.20
1	8	18.00	13.00	49.00	1.00	0.20
1	9	22.00	10.00	50.00	1.00	0.20
1	10	22.00	11.00	54.00	1.00	0.20
1	11	19.00	11.00	53.00	2.00	0.20
1	12	22.00	11.00	51.00	1.00	0.20
1	13	28.00	12.00	56.00	0.	0.20
1	14	31.00	9.00	59.00	1.00	0.20
1	15	27.00	12.00	57.00	0.	0.20
1	16	22.00	25.00	54.00	2.00	0.20
1	17	29.00	29.00	49.00	2.00	0.20
2	1	21.00	16.00	53.00	1.00	0.20
2	2	24.00	9.00	58.00	1.00	0.20
2	3	24.00	14.00	59.00	2.00	0.20
2	4	21.00	14.00	50.00	1.00	0.20
2	5	26.00	15.00	63.00	2.00	0.20
2	6	9.00	16.00	44.00	1.00	0.20
2	7	24.00	12.00	55.00	1.00	0.20
2	8	21.00	15.00	53.00	1.00	0.20
2	9	25.00	14.00	61.00	1.00	0.20
2	10	23.00	14.00	50.00	0.	0.20
2	11	21.00	14.00	52.00	2.00	0.20
2	12	26.00	14.00	59.00	2.00	0.20
2	13	24.00	15.00	54.00	1.00	0.20
2	14	23.00	12.00	55.00	1.00	0.20
2	15	32.00	12.00	57.00	1.00	0.20
2	16	31.00	9.00	58.00	0.	0.20
2	17	30.00	12.00	63.00	1.00	0.20
3	1	22.00	21.00	58.00	4.00	0.20
3	2	23.00	20.00	59.00	4.00	0.20
3	3	21.00	15.00	57.00	1.00	0.20
3	4	20.00	22.00	57.00	1.00	0.20
3	5	25.00	18.00	61.00	1.00	0.20
3	7	20.00	20.00	51.00	1.00	0.20
3	8	19.00	14.00	56.00	1.00	0.20
3	9	22.00	19.00	69.00	2.00	0.20
3	10	23.00	14.00	56.00	2.00	0.20
3	11	24.00	16.00	62.00	2.00	0.20
3	12	24.00	10.00	53.00	1.00	0.20
3	13	23.00	12.00	56.00	1.00	0.20
3	14	27.00	10.00	59.00	0.	0.20
3	15	19.00	14.00	48.00	1.00	0.20
3	16	29.00	10.00	58.00	0.	0.20
3	17	24.00	9.00	52.00	0.	0.20

EAST	NORTH	Cu	Pb	Zn	Mo	Ag
4	1	9.00	18.00	58.00	28.00	0.20
4	2	18.00	20.00	57.00	42.00	0.20
4	3	9.00	18.00	53.00	32.00	0.20
4	4	21.00	25.00	65.00	9.00	0.20
4	5	19.00	28.00	56.00	13.00	0.20
4	6	21.00	26.00	52.00	10.00	0.20
4	7	18.00	26.00	50.00	2.00	0.20
4	8	20.00	12.00	50.00	1.00	0.20
4	9	21.00	10.00	54.00	1.00	0.20
4	10	24.00	9.00	55.00	2.00	0.20
4	11	22.00	10.00	54.00	1.00	0.20
4	12	20.00	8.00	56.00	0.	0.20
4	13	22.00	8.00	50.00	1.00	0.20
4	14	20.00	10.00	48.00	0.	0.20
4	15	20.00	7.00	50.00	1.00	0.20
4	16	23.00	9.00	51.00	1.00	0.20
4	17	24.00	9.00	49.00	0.	0.20
5	1	18.00	20.00	56.00	15.00	0.20
5	2	13.00	18.00	46.00	21.00	0.20
5	3	16.00	20.00	50.00	25.00	0.20
5	4	15.00	23.00	49.00	18.00	0.20
5	5	15.00	9.00	52.00	33.00	0.20
5	6	18.00	33.00	63.00	44.00	0.30
5	7	13.00	70.00	54.00	35.00	0.40
5	8	19.00	25.00	52.00	12.00	0.20
5	9	20.00	18.00	53.00	2.00	0.30
5	10	19.00	20.00	51.00	2.00	0.20
5	11	9.00	16.00	49.00	0.	0.20
5	12	18.00	16.00	50.00	1.00	0.20
5	13	25.00	18.00	56.00	2.00	0.20
5	14	24.00	18.00	52.00	2.00	0.20
5	15	28.00	14.00	58.00	1.00	0.20
5	16	33.00	20.00	63.00	1.00	0.20
5	17	28.00	14.00	52.00	1.00	0.20
6	1	15.00	33.00	59.00	14.00	0.70
6	2	19.00	29.00	72.00	7.00	0.60
6	3	18.00	27.00	74.00	7.00	0.20
6	4	19.00	20.00	56.00	5.00	0.20
6	5	18.00	9.00	55.00	3.00	0.20
6	6	18.00	20.00	48.00	4.00	0.20
6	7	16.00	27.00	53.00	6.00	0.30
6	8	9.00	14.00	48.00	2.00	0.20
6	9	18.00	20.00	51.00	3.00	0.20
6	10	24.00	9.00	54.00	1.00	0.20
6	11	19.00	27.00	51.00	1.00	0.20
6	12	14.00	22.00	41.00	1.00	0.20
6	13	24.00	9.00	51.00	1.00	0.20
6	14	23.00	15.00	54.00	1.00	0.20
6	15	28.00	15.00	52.00	1.00	0.20
6	16	25.00	13.00	47.00	1.00	0.20

EAST	NORTH	Cu	Pb	Zn	Mo	Ag
6	17	25.00	14.00	48.00	2.00	0.20
7	1	16.00	18.00	65.00	2.00	0.20
7	2	11.00	37.00	72.00	7.00	0.30
7	3	10.00	16.00	55.00	12.00	0.20
7	4	9.00	9.00	44.00	14.00	0.20
7	5	9.00	12.00	33.00	5.00	0.20
7	6	12.00	18.00	90.00	9.00	0.20
7	7	13.00	9.00	39.00	5.00	0.20
7	8	14.00	21.00	35.00	3.00	0.30
7	9	20.00	9.00	51.00	1.00	0.20
7	10	13.00	19.00	54.00	3.00	0.20
7	11	23.00	16.00	54.00	3.00	0.20
7	12	25.00	12.00	51.00	1.00	0.20
7	13	25.00	20.00	53.00	1.00	0.20
7	14	26.00	10.00	47.00	0.	0.20
7	15	23.00	10.00	47.00	1.00	0.20
7	16	29.00	12.00	55.00	1.00	0.20
7	17	29.00	10.00	58.00	1.00	0.20
8	1	11.00	11.00	64.00	5.00	0.20
8	2	10.00	11.00	44.00	2.00	0.20
8	3	15.00	20.00	56.00	3.00	0.40
8	4	12.00	16.00	56.00	5.00	0.20
8	5	11.00	16.00	56.00	2.00	0.20
8	6	13.00	9.00	48.00	3.00	0.20
8	7	22.00	40.00	62.00	5.00	0.20
8	8	16.00	9.00	45.00	1.00	0.20
8	9	20.00	14.00	52.00	2.00	0.20
8	10	20.00	9.00	48.00	2.00	0.20
8	11	16.00	16.00	43.00	2.00	0.20
8	12	22.00	20.00	53.00	2.00	0.20
8	13	19.00	15.00	52.00	2.00	0.20
8	14	21.00	13.00	44.00	2.00	0.20
8	15	23.00	14.00	39.00	1.00	0.70
8	16	28.00	12.00	54.00	1.00	0.20
8	17	22.00	12.00	54.00	1.00	0.20
9	1	19.00	11.00	50.00	2.00	0.20
9	2	23.00	10.00	37.00	1.00	0.20
9	3	16.00	12.00	42.00	1.00	0.20
9	5	13.00	420.00	415.00	3.00	3.30
9	6	7.00	18.00	268.00	0.	0.20
9	7	20.00	16.00	55.00	2.00	0.20
9	8	20.00	11.00	44.00	0.	0.20
9	9	18.00	14.00	53.00	1.00	0.20
9	10	22.00	16.00	48.00	0.	0.20
9	11	23.00	9.00	49.00	0.	0.20
9	12	26.00	10.00	49.00	1.00	0.20
9	13	29.00	14.00	55.00	1.00	0.20
9	14	25.00	12.00	51.00	0.	0.20
9	15	27.00	10.00	53.00	1.00	0.20
9	16	24.00	14.00	57.00	1.00	0.20

EAST	NORTH	Cu	Pb	Zn	Mo	Ag
9	17	27.00	14.00	59.00	2.00	0.20
10	1	15.00	14.00	39.00	0.	0.20
10	2	19.00	14.00	56.00	1.00	0.20
10	3	9.00	16.00	57.00	2.00	0.20
10	4	10.00	16.00	61.00	0.	0.20
10	5	10.00	26.00	61.00	1.00	0.20
10	6	18.00	220.00	162.00	2.00	1.60
10	8	23.00	9.00	53.00	0.	0.20
10	9	22.00	10.00	49.00	0.	0.20
10	10	29.00	12.00	52.00	2.00	0.20
10	11	27.00	10.00	51.00	0.	0.20
10	12	26.00	10.00	48.00	0.	0.20
10	13	28.00	10.00	51.00	0.	0.20
10	14	33.00	11.00	60.00	1.00	0.20
10	15	26.00	11.00	51.00	2.00	0.20
10	16	25.00	14.00	57.00	3.00	0.20
10	17	25.00	13.00	58.00	3.00	0.20
11	1	22.00	8.00	51.00	0.	0.20
11	2	21.00	10.00	53.00	1.00	0.20
11	3	19.00	12.00	60.00	1.00	0.20
11	4	18.00	22.00	78.00	1.00	0.20
11	5	19.00	14.00	58.00	0.	0.20
11	6	10.00	28.00	86.00	1.00	0.20
11	7	23.00	650.00	132.00	1.00	3.40
11	8	21.00	22.00	59.00	0.	0.20
11	9	23.00	14.00	47.00	0.	0.20
11	10	25.00	13.00	49.00	0.	0.20
11	11	24.00	16.00	52.00	0.	0.20
11	12	30.00	16.00	54.00	0.	0.20
11	13	28.00	16.00	49.00	0.	0.20
11	14	22.00	13.00	47.00	1.00	0.20
11	15	23.00	14.00	51.00	1.00	0.20
11	16	24.00	18.00	58.00	3.00	0.20
11	17	18.00	30.00	52.00	2.00	1.20
12	1	26.00	10.00	56.00	1.00	0.20
12	2	9.00	10.00	48.00	1.00	0.20
12	3	21.00	8.00	50.00	0.	0.20
12	4	23.00	10.00	52.00	0.	0.20
12	5	24.00	11.00	51.00	0.	0.20
12	6	29.00	10.00	47.00	0.	0.20
12	7	22.00	12.00	52.00	1.00	0.20
12	8	26.00	20.00	55.00	0.	0.20
12	13	27.00	15.00	58.00	1.00	0.20
12	14	16.00	14.00	47.00	2.00	0.20
12	15	13.00	16.00	48.00	1.00	0.20
12	16	16.00	15.00	57.00	2.00	0.20
12	17	19.00	15.00	51.00	1.00	0.20
13	1	28.00	14.00	54.00	1.00	0.20
13	2	26.00	14.00	58.00	1.00	0.20
13	3	26.00	12.00	55.00	0.	0.20

EAST	NORTH	Cu	Pb	Zn	Mo	Ag
13	4	24.00	14.00	52.00	0.	0.20
13	5	18.00	16.00	50.00	0.	0.20
13	6	13.00	24.00	49.00	0.	0.20
13	7	23.00	28.00	62.00	0.	0.20
13	8	18.00	14.00	58.00	0.	0.40
13	13	14.00	84.00	46.00	0.	3.00
13	14	13.00	43.00	48.00	1.00	1.00
13	15	14.00	22.00	52.00	3.00	0.40
13	16	14.00	26.00	47.00	2.00	0.40
13	17	11.00	20.00	53.00	2.00	0.30
14	1	22.00	10.00	48.00	1.00	0.20
14	2	23.00	27.00	58.00	1.00	0.50
14	3	27.00	12.00	54.00	2.00	0.20
14	4	18.00	12.00	54.00	2.00	0.20
14	5	10.00	23.00	43.00	2.00	0.20
14	6	15.00	48.00	99.00	2.00	0.20
14	9	27.00	38.00	61.00	1.00	0.20
14	10	14.00	26.00	63.00	0.	0.20
14	11	16.00	20.00	50.00	0.	0.20
14	12	13.00	34.00	72.00	1.00	0.20
14	13	15.00	70.00	62.00	1.00	0.20
14	14	9.00	40.00	103.00	0.	0.20
14	15	9.00	21.00	22.00	0.	0.20
14	16	11.00	21.00	34.00	0.	0.20
14	17	12.00	20.00	54.00	1.00	0.20
15	1	24.00	12.00	52.00	0.	0.20
15	2	21.00	13.00	48.00	1.00	0.20
15	3	12.00	32.00	52.00	2.00	0.30
15	4	30.00	12.00	63.00	2.00	0.20
15	5	16.00	16.00	61.00	1.00	0.20
15	6	11.00	19.00	77.00	18.00	0.20
15	7	15.00	72.00	82.00	2.00	0.90
15	8	12.00	18.00	43.00	0.	0.20
15	9	21.00	22.00	64.00	1.00	0.20
15	10	13.00	27.00	54.00	2.00	0.20
15	11	21.00	20.00	60.00	0.	0.20
15	12	18.00	26.00	78.00	0.	0.20
15	13	16.00	30.00	73.00	0.	0.20
15	14	14.00	30.00	63.00	1.00	0.90
15	15	15.00	15.00	45.00	0.	0.20
15	16	12.00	58.00	75.00	2.00	0.20
15	17	14.00	42.00	56.00	2.00	0.60
16	1	21.00	10.00	52.00	0.	0.20
16	2	19.00	10.00	44.00	0.	0.20
16	3	25.00	12.00	57.00	0.	0.20
16	4	20.00	11.00	48.00	1.00	0.20
16	5	22.00	14.00	58.00	0.	0.20
16	6	12.00	12.00	29.00	0.	0.30
16	9	16.00	98.00	131.00	1.00	0.90
16	10	15.00	19.00	58.00	1.00	0.20

EAST	NORTH	Cu	Pb	Zn	Mo	Ag
16	11	11.00	14.00	44.00	1.00	0.20
16	12	15.00	14.00	47.00	1.00	0.20
16	13	13.00	40.00	63.00	3.00	0.20
16	14	16.00	50.00	65.00	1.00	0.20
16	15	10.00	29.00	61.00	1.00	0.20
16	16	11.00	22.00	47.00	0.	0.20
16	17	10.00	43.00	48.00	2.00	0.40

APPENDIX D

Corrected geomagnetic data from the
geochemical-survey grid (all values in gammas).

EAST	NORTH	GAMMAS
1	1	55483
1	2	55485
1	3	55486
1	4	55485
1	5	55491
1	6	55493
1	7	55491
1	8	55473
1	9	55482
1	10	55479
1	11	55480
1	12	55482
1	13	55483
1	14	55489
1	15	55486
1	16	55485
1	17	55474
1	18	55477
1	19	55475
1	20	55476
1	21	55480
1	22	55480
1	23	55482
1	24	55479
1	25	55480
1	26	55477
1	27	55481
1	28	55482
1	29	55484
1	30	55485
1	31	55489
1	32	55488
1	33	55475
3	1	55502
3	2	55501
3	3	55502
3	4	55502
3	5	55496
3	6	55494
3	7	55496
3	8	55496
3	9	55485
3	11	55506
3	12	55496
3	13	55508
3	14	55506
3	15	55509
3	16	55505
3	17	55506
3	18	55542

EAST	NORTH	GAMMAS
3	19	55544
3	20	55550
3	21	55551
3	22	55555
3	23	55554
3	24	55555
3	25	55555
3	26	55556
3	27	55555
3	28	55546
3	29	55541
3	30	55541
3	31	55547
3	32	55546
3	33	55555
4	1	55499
4	2	55489
4	3	55501
4	4	55499
4	5	55504
4	6	55499
4	7	55505
4	8	55500
4	9	55500
4	10	55504
4	11	55501
4	12	55506
4	13	55494
4	14	55497
4	15	55502
4	16	55510
4	17	55514
4	18	55513
4	19	55509
4	20	55512
4	21	55512
4	22	55509
4	23	55514
4	24	55508
4	25	55507
4	26	55511
4	28	55504
4	29	55512
4	30	55497
4	31	55500
4	32	55505
4	33	55517
5	1	55529
5	2	55504
5	3	55505

EAST	NORTH	GAMMAS
5	4	55496
5	5	55508
5	6	55505
5	7	55501
5	8	55498
5	9	55501
5	10	55506
5	11	55496
5	14	55509
5	15	55500
5	16	55503
5	17	55510
5	18	55508
5	19	55505
5	20	55499
5	21	55506
5	22	55508
5	23	55500
5	24	55513
5	25	55504
5	26	55505
5	27	55509
5	28	55508
5	29	55514
5	30	55507
5	31	55511
5	32	55512
5	33	55502
6	1	55506
6	2	55505
6	3	55511
6	4	55509
6	5	55512
6	6	55515
6	7	55512
6	8	55509
6	9	55510
6	10	55509
6	11	55505
6	12	55508
6	13	55509
6	14	55514
6	15	55514
6	16	55515
6	17	55513
6	18	55526
6	19	55517
6	20	55521
6	21	55523
6	22	55520

EAST	NORTH	GAMMAS
6	23	55522
6	24	55520
6	25	55522
6	26	55525
6	27	55518
6	28	55518
6	29	55523
6	30	55526
6	31	55522
6	32	55521
6	33	55522
7	1	55518
7	2	55522
7	3	55511
7	4	55512
7	5	55516
7	6	55515
7	7	55512
7	8	55514
7	9	55505
7	10	55519
7	12	55506
7	13	55507
7	14	55505
7	15	55509
7	16	55510
7	17	55514
7	18	55513
7	19	55518
7	20	55509
7	21	55520
7	22	55513
7	23	55511
7	24	55516
7	25	55513
7	26	55509
7	27	55510
7	28	55507
7	29	55508
7	30	55509
7	31	55514
7	32	55513
7	33	55514
8	1	55519
8	2	55523
8	3	55533
8	4	55527
8	5	55521
8	6	55517
8	7	55522

EAST	NORTH	GAMMAS
8	8	55520
8	9	55516
8	10	55515
8	11	55513
8	12	55508
8	13	55510
8	14	55503
8	15	55504
8	16	55513
8	17	55503
8	18	55514
8	19	55502
8	20	55508
8	21	55517
8	22	55512
8	23	55514
8	24	55514
8	25	55514
8	26	55514
8	27	55512
8	28	55510
8	29	55512
8	30	55511
8	31	55519
8	32	55513
8	33	55511
9	1	55510
9	2	55514
9	3	55517
9	4	55514
9	5	55514
9	6	55521
9	7	55513
9	8	55518
9	9	55506
9	10	55491
9	11	55512
9	12	55514
9	13	55524
9	14	55517
9	15	55509
9	16	55516
9	17	55516
9	18	55504
9	19	55508
9	20	55516
9	21	55515
9	22	55512
9	23	55512
9	24	55510

EAST	NORTH	GAMMAS
9	25	55512
9	26	55506
9	27	55511
9	28	55508
9	29	55510
9	30	55507
9	31	55507
9	32	55515
9	33	55533
10	1	55456
10	2	55461
10	3	55459
10	4	55460
10	5	55459
10	6	55462
10	7	55472
10	8	55415
10	9	55410
10	10	55420
10	11	55413
10	12	55380
10	13	55407
10	14	55398
10	15	55435
10	16	55407
10	17	55455
10	18	55499
10	19	55508
10	20	55499
10	21	55507
10	22	55509
10	23	55508
10	24	55507
10	25	55505
10	26	55507
10	27	55506
10	28	55502
10	29	55506
10	30	55504
10	31	55512
10	32	55513
10	33	55484
11	1	55550
11	2	55491
11	3	55493
11	4	55498
11	5	55500
11	6	55502
11	7	55500
11	8	55503

EAST	NORTH	GAMMAS
11	9	55500
11	10	55498
11	11	55504
11	12	55497
11	13	55496
11	14	55496
11	15	55503
11	16	55496
11	17	55505
11	18	55518
11	19	55505
11	20	55515
11	21	55512
11	22	55513
11	23	55514
11	24	55516
11	25	55530
11	26	55517
11	27	55514
11	28	55512
11	29	55507
11	30	55496
11	31	55515
11	32	55508
11	33	55503
12	1	55488
12	2	55495
12	3	55498
12	4	55508
12	5	55491
12	6	55501
12	7	55506
12	8	55516
12	9	55516
12	10	55516
12	11	55527
12	12	55526
12	13	55530
12	14	55527
12	15	55500
12	16	55513
12	17	55528
12	18	55499
12	19	55494
12	20	55501
12	21	55503
12	22	55502
12	23	55512
12	24	55491
12	25	55496
12	26	55506
12	27	55504
12	28	55500
12	29	55483
12	30	55499
12	31	55514
12	32	55502
12	33	55499
13	1	55477
13	2	55489
13	3	55488
13	4	55489
13	5	55492
13	6	55494
13	7	55494
13	8	55499
13	9	55505
13	10	55507
13	11	55500
13	12	55494
13	13	55501
13	14	55507
13	15	55511
13	16	55508
13	17	55501
13	18	55495
13	19	55496
13	20	55499
13	21	55495
13	22	55511
13	23	55486
13	24	55499
13	25	55493
13	26	55489
13	27	55498
13	28	55494
13	29	55496
13	30	55500
13	31	55496
13	32	55488
13	33	55507
14	1	55469
14	2	55480
14	3	55487
14	4	55490
14	5	55493
14	6	55493
14	7	55489
14	8	55495
14	9	55495

EAST	NORTH	GAMMAS
14	10	55500
14	11	55473
14	12	55495
14	13	55501
14	14	55496
14	15	55498
14	16	55493
14	17	55491
14	18	55500
14	19	55498
14	20	55501
14	21	55502
14	22	55502
14	23	55499
14	24	55495
14	25	55493
14	26	55488
14	27	55495
14	28	55484
14	29	55500
14	30	55489
14	31	55487
14	32	55494
14	33	55488
15	1	55459
15	2	55472
15	3	55468
15	4	55477
15	5	55474
15	6	55464
15	7	55472
15	8	55482
15	9	55475
15	10	55471
15	11	55450
15	13	55459
15	14	55459
15	15	55495
15	16	55496
15	17	55493
15	18	55498
15	19	55498
15	20	55498
15	21	55495
15	22	55505
15	23	55498
15	24	55500
15	25	55495
15	26	55504
15	27	55506

EAST	NORTH	GAMMAS
15	28	55506
15	29	55497
15	30	55497
15	31	55495
15	32	55490
15	33	55501
16	1	55463
16	2	55464
16	3	55473
16	4	55477
16	5	55483
16	6	55481
16	7	55483
16	8	55487
16	9	55491
16	10	55497
16	11	55502
16	12	55501
16	18	55508
16	19	55506
16	20	55516
16	21	55505
16	22	55514
16	23	55512
16	24	55503
16	25	55511
16	26	55507
16	27	55499
16	28	55503
16	29	55494
16	30	55504
16	31	55502
16	32	55502
16	33	55495